AD_____

Award Number: DAMD17-03-1-0672

TITLE: MUC1 Functions as an Oncogene by Targeting the Nucleus of Human Breast Cancer Cells

PRINCIPAL INVESTIGATOR: Donald Kufe, M.D.

CONTRACTING ORGANIZATION: Dana-Farber Cancer Institute
Boston, MA 02115

REPORT DATE: September 2005

TYPE OF REPORT: Annual

PREPARED FOR: U.S. Army Medical Research and Materiel Command
Fort Detrick, Maryland 21702-5012

DISTRIBUTION STATEMENT: Approved for Public Release;
Distribution Unlimited

REPORT DOCUMENTATION PAGE

Form Approved
OMB No. 0704-0188

1. REPORT DATE *(DD-MM-YYYY)*	2. REPORT TYPE	3. DATES COVERED *(From - To)*
01-09-2005	Annual	1 Sep 04 – 31 Aug 05

4. TITLE AND SUBTITLE
MUC1 Functions as an Oncogene by Targeting the Nucleus of Human Breast Cancer Cells

5a. CONTRACT NUMBER

5b. GRANT NUMBER
DAMD17-03-1-0672

5c. PROGRAM ELEMENT NUMBER

6. AUTHOR(S)
Donald Kufe, M.D.

E-Mail: Donald_kufe@dfci.harvard.edu

5d. PROJECT NUMBER

5e. TASK NUMBER

5f. WORK UNIT NUMBER

7. PERFORMING ORGANIZATION NAME(S) AND ADDRESS(ES)
Dana-Farber Cancer Institute
Boston, MA 02115

8. PERFORMING ORGANIZATION REPORT NUMBER

9. SPONSORING / MONITORING AGENCY NAME(S) AND ADDRESS(ES)
U.S. Army Medical Research and Materiel Command
Fort Detrick, Maryland 21702-5012

10. SPONSOR/MONITOR'S ACRONYM(S)

11. SPONSOR/MONITOR'S REPORT NUMBER(S)

12. DISTRIBUTION / AVAILABILITY STATEMENT
Approved for Public Release; Distribution Unlimited

13. SUPPLEMENTARY NOTES

14. ABSTRACT

Abstract is attached at the following page.

15. SUBJECT TERMS
MUC1, transformation, nuclear localization, gene expression, cell proliferation

16. SECURITY CLASSIFICATION OF:			17. LIMITATION OF ABSTRACT	18. NUMBER OF PAGES	19a. NAME OF RESPONSIBLE PERSON
a. REPORT	b. ABSTRACT	c. THIS PAGE			USAMRMC
U	U	U	UU	58	19b. TELEPHONE NUMBER *(include area code)*

ABSTRACT

The MUC1 oncoprotein is aberrantly overexpressed in 80-90% of human breast carcinomas. Little, however, is known about the role of MUC1 in the development of breast cancer. The Specific Aims of this Idea Award are: 1) To determine if MUC1 overexpression is sufficient to induce transformation; and 2) To assess whether MUC1 localizes to the nucleus and thereby regulates gene expression. Work supported by this Award has demonstrated that the MUC1 cytoplasmic domain (MUC1-CD) is sufficient to induce transformation and that the oncogenic effects of MUC1 are mediated at least in part by stabilization of the Wnt effector β-catenin. Our work has also shown that MUC1 interacts with the p53 tumor suppressor and contributes to the regulation of p53-dependent transcription. More recent studies show that MUC1 binds to estrogen receptor α (ERα) and that MUC1 increases ERα levels by blocking its ubiquitination and degradation. MUC1 occupies the promoters of estrogen responsive genes and activates ERα-mediated transcription. These findings indicate that MUC1 induces transformation, localizes to the nucleus and regulates gene expression in breast cancer cells.

Table of Contents

INTRODUCTION

The MUC1 transmembrane glycoprotein is normally expressed on the apical borders of secretory mammary epithelia (1). With transformation and loss of polarity, MUC1 is aberrantly overexpressed in the cytosol and on the entire surface of breast cancer cells (1, 2). The MUC1 locus has been mapped to human chromosome 1q21 in a region that is frequently affected by genetic alterations in breast and other carcinomas (3, 4). MUC1 is expressed as a stable heterodimer following translation of a single polypeptide and cleavage into two subunits in the endoplasmic reticulum (5). The MUC1 N-terminal subunit (MUC1 N-ter, MUC1-N) contains variable numbers of 20 amino acid tandem repeats that are extensively modified by O-linked glycans (6, 7). The MUC1 C-terminal subunit (MUC1 C-ter, MUC1-C) consists of a 58 amino acid extracellular domain, a 28 amino acid transmembrane domain and a 72 amino acid cytoplasmic tail (4). On the cell surface, MUC1-N extends well beyond the glycocalyx and is tethered by MUC1-C to the cell membrane. MUC1-C also accumulates in the cytosol of transformed cells and is targeted to the nucleus (8-11) and mitochondria (12). The MUC1 cytoplasmic domain (MUC1-CD) associates with members of the catenin family (13, 14) and with the p53 tumor suppressor (15). MUC1-CD is also subject to phosphorylation by the epidermal growth factor receptor (EGFR) (16), c-Src (17) and glycogen synthase kinase 3β (GSK3β) (18). The finding that MUC1 interacts with ErbB2 has further supported a role for MUC1 in both the ErbB receptor tyrosine kinase and Wnt signaling pathways (10, 19). Of potential importance to the aberrant regulation of MUC1 in breast carcinomas, other studies have shown that MUC1 overexpression is sufficient to confer anchorage-independent growth and tumorigenicity (9, 20-22).

Most human breast cancers are estrogen dependent and their treatment with estrogen antagonists, particularly tamoxifen, has had a dramatic effect on mortality (23). Estrogen action is mediated by two members of the nuclear receptor family, estrogen receptor α (ERα) and ERβ. Both ERs contain a central DNA-binding domain (DBD), which binds to estrogen response elements (EREs), and a C-terminal ligand binding domain (LBD). ERα and ERβ have substantial

homology in their DBDs and thus may regulate common sets of genes. However, in contrast to ERβ knockout mice, ERα knockout mice are infertile, supporting different roles for these receptors (24, 25). Upon estrogen binding, ERα undergoes conformational changes and dimerization that confer binding to EREs. Activation of ERα-mediated transcription is regulated by activation function-1 (AF-1) in the N-terminal region and AF-2 in the LBD. AF-1 is activated by growth factors through the MAP kinase pathway (26), and AF-2 is activated by binding of estrogen (27). In the response to estrogen, ERα transcription complexes on target promoters recruit coactivators from i) the p160 family (SRC-1/NCoA-1, GRIP1/NCoA-2 and AIB1/RAC3/ACTR) (28, 29), ii) non-p160 proteins (RIP140, mSUG1 and TIF1) (30-32), and iii) histone acetylases (p300 and CBP) and the p300/CBP-associated factor pCAF (33). The structural changes induced by binding of estrogen to the ERα LBD promotes the recruitment of p160 coactivators (34). ERα also interacts with basal transcription factors to increase the initiation of transcription (35, 36). Notably, recruitment of p160 coactivators is sufficient for ERα-mediated gene activation and for estrogen-induced growth stimulation (37). By contrast, tamoxifen competes with estrogen for binding to ERα and induces conformational changes that block recruitment of coactivators (37, 38). In addition, tamoxifen bound ERα recruits corepressors to estrogen responsive-promoters (37).

The overexpression of MUC1 in most human breast carcinomas, the correlation between MUC1 and ERα levels in breast tumors (39) and the importance of ERα for breast cancer cell growth prompted us to investigate whether MUC1 interacts with ERα. The results demonstrate that MUC1 binds directly to the ERα DBD and stabilizes ERα. We also show that MUC1 is present in the ERα transcription complex, stimulates ERα-mediated transcription and promotes E2-mediated growth and survival of breast cancer cells.

BODY

MUC1 associates with ERα. Human MCF-7 breast cancer cells were studied to determine if MUC1 interacts with ERα. In MCF-7 and other cell types, the MUC1 C-terminal subunit (MUC1-C) is expressed as a ~20-25 kDa protein and to a lesser extent as ~17-12 kDa fragments. Immunoblot analysis of anti-ERα immunoprecipitates with an antibody that reacts with the MUC1 cytoplasmic domain (MUC1-CD) demonstrated that ERα coprecipitates with MUC1-C (Fig. 1A). As a control, there was no detectable MUC1-C in precipitates prepared with IgG (Fig. 1A). The results also demonstrate that the association between ERα and MUC1-C is increased by 17β-estradiol (E2) stimulation (Fig. 1A). Similar studies performed with ZR-75-1 breast cancer cells confirmed that ERα associates with MUC1-C and that the association is stimulated by E2 (Fig. 1B). A kinetic analysis of the interaction showed that MUC1-ERα complexes increase at 3 to 6 h of E2 stimulation and then decline at 12 and 24 h (Supplemental Figs. S1A and B). Densitometric scanning of the MUC1 signals obtained from whole cell lysates as compared to that after immunoprecipitation of the lysates with anti-ERα indicate that ~3 and 5% of the total MUC1-C associates with ERα in control and E2-stimulated MCF-7 cells, respectively (Supplemental Fig. S1C). In ZR-75-1 cells, ~4 and 6% of total MUC1-C associated with ERα in the absence and presence of E2, respectively (Supplemental Fig. S1D). As a control, cell lysates were immunoprecipitated with an antibody against the proliferating cell nuclear antigen (PCNA). There was no detectable MUC1-C in the anti-PCNA precipitates from MCF-7 (Supplemental Fig. S1E) or ZR-75-1 (Supplemental Fig. S1F) cells. To define the region of MUC1-C responsible for the interaction, Myc-tagged MUC1 cytoplasmic domain (Myc-MUC1-CD) was coexpressed with ERα in COS-1 cells. Immunoblot analysis of anti-ERα precipitates with anti-MUC1-CD demonstrated that MUC1-CD is sufficient for the association with ERα (Fig. 1C). Moreover, stimulation of the COS-1 cells with E2 increased binding of ERa and Myc-MUC1-CD (Fig. 1C). This association was confirmed in the reciprocal experiment in which anti-Myc immunoprecipitates were immunoblotted with anti-ERa (Fig. 1D). These findings indicate that MUC1 associates with ERα constitutively and that this interaction is increased in the response to E2.

MUC1-CD binds directly to ERα. To define the regions of MUC1-CD (72 amino acids) and ERα (595 amino acids) responsible for the interaction (Fig. 2A), GST or a GST-MUC1-CD fusion protein was incubated with ^{35}S-labeled ERa in vitro. Analysis of adsorbates to glutathione beads demonstrated binding of full-length ERα(1-595) to GST-MUC1-CD and not GST (Fig. 2B). By contrast, there was no detectable binding of MUC1-CD to ERα(1-185) that contains the AF1 domain (Fig. 2B). Moreover, the demonstration that MUC1-CD binds to ERα(1-282) indicated involvement of the DNA binding domain (DBD) (Fig. 2B). Consistent with these results, binding of MUC1-CD was found with ERα(185-595), but not ERα(282-595) or ERα(Δ186-281) devoid of the DBD (Fig. 2B). Binding was also observed with ERα(186-281), confirming that MUC1-CD interacts directly with the ERα DBD (Fig. 2C). To localize the region within MUC1-CD that interacts with ERα, ^{35}S-labeled full length ERα was incubated with deletion mutants of MUC1-CD. The results demonstrate that ERα binds to both full-length MUC1-CD and MUC1-CD(1-51), indicating that the N-terminal region of MUC1-CD is sufficient for the interaction (Fig. 2D). Consistent with those results, deletion of MUC1-CD amino acids 9 to 46 abrogated the association with ERα (Fig. 2D). Binding in vitro was also compared in the absence and presence of E2. The results show an E2-dependent increase in the binding of MUC1-CD and full-length ERα (Fig. 2E). By contrast, 4-hydroxytamoxifen (TAM) had no apparent effect on the formation of MUC1-CD-ERα complexes (Fig. 2E). These findings indicate that MUC1-CD(9-46) binds directly to the ERα DBD and that this interaction is stimulated by E2.

MUC1 stabilizes ERα. To assess the effects of MUC1 on ERα expression, MCF-7 cells were stably infected with a retrovirus expressing MUC1siRNA. Immunoblot analysis of two separately isolated clones demonstrated partial (~80-90%) and complete down-regulation of MUC1 in MCF-7/MUC1siRNA-A and MCF-7/MUC1siRNA-B cells, respectively, as compared to that in cells expressing a control siRNA (CsiRNA) (Supplemental Fig. S2A). Assessment of ERα levels in the MCF-7, MCF-7/CsiRNA and MCF-7/MUC1siRNA cells demonstrated that knocking-down

MUC1 is associated with decreases in ERα expression (Fig. 3A, left). Densitometric scanning of the ERα signals in independent experiments and at different levels of exposure demonstrated that MUC1 increases ERα levels by 2.9±0.5-fold (mean±SD of three experiments) (Supplemental Fig. S2B). Compared with MCF-7 cells, ERα expression was lower in ZR-75-1 cells (Supplemental Fig. S2C). Moreover, silencing MUC1 in ZR-75-1 cells (Supplemental Fig. S2D) was associated with decreases in ERα expression (Fig. 3A, right). Quantification of the ERα signals in independent experiments and at different levels of exposure showed that MUC1 increases ERα levels by 4.0±0.6-fold (mean±SD of three experiments) in ZR-75-1 cells (Supplemental Fig. S2E). Semiquantitative RT-PCR analysis of the MCF-7 and ZR-75-1 cells demonstrated that ERα mRNA levels are similar in the presence and absence of MUC1 (Supplemental Figs. S3A and B), indicating that MUC1 regulates ERα by a post-translational mechanism. In this regard, stability of the ERα protein is controlled by ubiquitination and proteosomal degradation (40-42). Consequently, ERα levels were assessed in the response of MCF-7 and ZR-75-1 cells to the proteosomal inhibitor MG132. Inhibition of the proteosome was associated with increases in ERα expression and this effect was more pronounced in cells silenced for MUC1 (Fig. 3B). Immunoblot analysis of anti-ERα precipitates with anti-ubiquitin (Ub) further showed that downregulation of MUC1 in MCF-7 cells is associated with increased ubiquitination of ERα (Fig. 3C, left). Similar results were obtained in ZR-75-1 cells (Fig. 3C, right). To further assess the effects of MUC1 on ERα stability, cells were pulsed with [^{35}S]-methionine and ERα was immunoprecipitated at various intervals during the chase period. Analysis of ERα by autoradiography showed that the half-life of ERα is decreased in the absence of MUC1 in both MCF-7 (Fig. 3D) and ZR-75-1 (Supplemental Fig. S3C) cells. The estrogen antagonist ICI182,780 (ICI) targets ERα to the proteosome (42, 43). Consistent with a role for MUC1 in stabilizing ERα, ICI-induced down-regulation of ERα was attenuated in the presence of MUC1 (Supplemental Fig. S3D). These findings indicate that MUC1 stabilizes ERα by blocking its ubiquitination and proteosomal degradation.

MUC1 occupies estrogen-responsive gene promoters. To determine if MUC1 is present in the ERα transcription complex, we performed chromatin immunoprecipitation (ChIP) assays with anti-MUC1-C. Immunoprecipitation of the estrogen-responsive region in the promoter of the pS2 gene (-353 to –30) (44) was analyzed by semiquantitative PCR. In both MCF-7 and ZR-75-1 cells, occupancy of the pS2 promoter by MUC1 was detectable in the absence of E2 and was increased by E2 stimulation (Fig. 4A). As controls, there were no detectable pS2 promoter sequences in immunoprecipitates performed with IgG (Fig. 4A). There was also no detectable MUC1 associated with a control region (CR; -2446 to –2125) of the pS2 promoter upstream to the ERE (Fig. 4A). The chromatin immunoprecipitates were further analyzed for the estrogen-responsive region (-295 to –54) of the cathepsin D gene promoter (45). As found for the pS2 promoter, MUC1 occupancy of the cathepsin D promoter in MCF-7 cells was detectable constitutively and was increased by E2 stimulation (Fig. 4B). By contrast, MUC1 occupancy was not detectable in a control region (CR; -4346 to –4105) of the cathepsin D promoter (Fig. 4B). Similar results were obtained in ZR-75-1 cells (Fig. 4B). To assess whether MUC1 occupies the pS2 promoter with ERα, the anti-MUC1 complexes were released, re-immunoprecipitated with anti-ERα and then analyzed by PCR (Re-ChIP). As shown for both MCF-7 and ZR-75-1 cells, anti-ERα precipitated the pS2 promoter after release from anti-MUC1, indicating that MUC1 is present in the region occupied by the ERα transcription complex (Fig. 4C). The results also demonstrate that the cathepsin D promoter is immunoprecipitated with anti-ERα after release from anti-MUC1 (Fig. 4D). In concert with the demonstration that E2 stimulates binding of ERα and MUC1, the Re-ChIP assays further showed that E2 increases complexes of ERα and MUC1 on the pS2 and cathepsin D promoters (Figs. 4C and D). The kinetics of MUC1 occupancy of the EREs was also assessed by performing ChIPs at different intervals of E2 stimulation. As found previously (37, 42, 46-48), ERα occupancy of the pS2 and cathepsin D EREs was detectable at low levels in the absence of E2 and was increased with E2 stimulation (Fig. 4E). Like ERα, increases in MUC1 occupancy of the pS2 and cathepsin D EREs were detectable at 15 to 30 min of E2 exposure (Fig. 4E). Moreover, maximal occupancy for both MUC1 and ERα was observed

when the cells were stimulated with E2 for 1 and 3 h (Fig. 4E). Other studies have reported that ERα occupancy of EREs is cyclical following E2 stimulation (47). The absence of apparent ERα cycling in the present studies is probably due to different experimental conditions; for example, use of a 10-fold higher E2 concentration, no a-amanitin release and less frequent sampling. To determine if MUC1 occupancy of EREs is dependent on ERα, human MDA-MB-231 breast cancer cells, which are negative for MUC1 and ERα, were stably transfected to express an empty vector or MUC1 (Supplemental Figs. S4A and S4B). The MDA-MB-231/MUC1 transfectants expressed MUC1 at levels comparable to that in ZR-75-1 cells (Supplemental Fig. S4A). The MDA-MB-231/vector and MDA-MB-231/MUC1 cells were also transiently transfected to express ERα (Supplemental Fig. S4B). Compared to MCF-7 cells, MUC1 occupancy of the pS2 and cathepsin D EREs was substantially decreased in the MDA-MB-231/MUC1 cells (Supplemental Fig. S4C). Moreover, MUC1 occupancy of the pS2 and cathepsin D EREs was markedly increased by transfection of ERα (Supplemental Fig. S4C). These findings indicate that i) MUC1 is a component of the ERα transcription complex, ii) E2 stimulation is associated with increases in occupancy of both ERα and MUC1 on EREs, and iii) MUC1 occupancy of EREs is dependent on ERα.

MUC1 activates ERα-mediated transcription. ChIP assays performed on the MCF-7/CsiRNA and MCF-7/MUC1siRNA-A cells showed that ERα occupancy of the pS2 promoter is decreased by knocking-down MUC1 expression (Fig. 5A, left). As expected, E2 stimulation was associated with increased occupancy of the pS2 promoter by ERα; however, this response was attenuated in the MCF-7/MUC1siRNA cells (Fig. 5A, left). Similar effects of MUC1 were observed when analyzing the cathepsin D promoter (Fig. 5A, right). As a control, silencing MUC1 decreased MUC1 occupancy of the pS2 and cathepsin D promoters (Supplemental Fig. S5A). Densitometric scanning of the signals obtained from multiple experiments also showed that MUC1 increased ERα occupancy of the pS2 and cathepsin D promoters by ~2-fold in the presence of ligand (Supplemental Fig. S5B). To assess the effects of MUC1 on ERα-mediated

transcription, the MCF-7/CsiRNA and MCF-7/MUC1siRNA-A cells were transfected with an ERE-tk-Luc reporter and then stimulated with E2. MUC1 expression was associated with little if any activation of the ERE promoter in the absence of E2 stimulation (Fig. 5B). By contrast, MUC1-dependent activation of ERE-tk-Luc was increased ~5-fold when the cells were stimulated with E2 (Fig. 5B). Further increases in MUC1-dependent stimulation of ERα-mediated transcription were found when the MCF-7 cells were transfected with different amounts of the ERα vector (Fig. 5B). To determine if MUC1 exhibits similar effects in ZR-75-1 cells, we used ZR-75-1/vector and ZR-75-1/MUC1siRNA cells (12). Knocking-down MUC1 expression in ZR-75-1 cells decreased ERα occupancy of the pS2 promoter in both the absence and presence of E2 stimulation (Fig. 5C, left). Similar results were obtained when analyzing the cathepsin D ERE (Fig. 5C, right). As found in MCF-7 cells, silencing MUC1 in ZR-75-1 cells decreased MUC1 occupancy of the pS2 and cathepsin D promoters (Supplemental Fig. S5C). Quantitation of the ERa signals showed that MUC1 increases ERα occupancy of the pS2 and cathepsin D promoters by ~2-fold in the presence of ligand (Supplemental Fig. S5D). Silencing MUC1 in ZR-75-1 cells also decreased E2-mediated activation of the ERE-tk-Luc reporter (Fig. 5D). These findings indicate that MUC1 increases ERα occupancy of EREs and ERα-mediated transcription.

MUC1 increases occupancy of p160 coactivators on estrogen-responsive promoters. To determine if MUC1-dependent stabilization of ERα affects recruitment of transcriptional coactivators, we asked if MUC1 occupies EREs with the p160 family members, SRC-1 and GRIP1. In Re-ChIP assays performed on MCF-7 cells, release of anti-MUC1 immunoprecipitates and re-precipitation with anti-SRC-1 demonstrated that SRC-1 is present in MUC1 complexes on both the pS2 and cathepsin D promoters (Fig. 6A, upper panels). Similar results were obtained when the Re-ChIP assays were performed on soluble chromatin from ZR-75-1 cells (Fig. 6A, upper panels). Also, in both cells, promoter complexes of MUC1 and SRC-1 were increased by E2 stimulation (Fig. 6A, upper panels). The results of Re-ChIP assays further showed that MUC1 is present with GRIP1 on the pS2 and cathepsin D promoters and that these

complexes are increased by E2 (Fig. 6A, lower panels). By contrast, there was no detectable MUC1 associated with control regions of the pS2 and cathepsin D promoters that are upstream to the EREs (Fig. 6A). To further assess the effects of MUC1 on coactivator occupancy of EREs, ChIP assays were performed on the MCF-7/CsiRNA and MCF-7/MUC1siRNA cells. Occupancy of the pS2 and cathepsin D promoter by SRC-1 was more pronounced in the MUC1-positive cells in both the absence and presence of E2 stimulation (Fig. 6B, upper panels). Similar results were obtained for GRIP1 occupancy (Fig. 6B, upper panels). Moreover, TAM was substantially more effective in decreasing SRC-1/GRIP1 occupancy of the pS2 and cathepsin D promoters in MCF-7 cells with downregulation of MUC1 expression (Fig. 6B, upper panels). Consistent with these findings, down-regulation of E2-induced transcription by TAM was attenuated in MCF-7/CsiRNA, as compared to that in MCF-7/MUC1siRNA, cells (Fig. 6B, lower panel). Our in vivo studies were performed at saturating levels of E2 (37). Whole MCF-7 cell binding assays demonstrated that saturation with [^{3}H]-E2 occurs at an approximately 2-fold higher level in the presence of MUC1, consistent with MUC1-induced increases in ERα (Supplemental Fig. S6A). At a 10-fold molar excess of TAM to E2 as used in the transcription studies, [^{3}H]-E2 saturation was decreased by ~40% in both MCF-7/CsiRNA and MCF-7/MUC1siRNA cells (Supplemental Fig. S6A). Thus, with the addition of TAM, ERa/E2 complexes remained ~2-fold higher in the presence of MUC1 (Supplemental Fig. S6A). Scatchard analysis of the binding data further demonstrated equilibrium dissociation constants (Kd) values that are similar in the absence and presence of MUC1, indicating that silencing MUC1 has little if any effect on ligand binding affinity (Supplemental Fig. S6B). TAM-induced decreases of SRC-1/GRIP1 occupancy on the pS2 and cathepsin D promoters were also attenuated by MUC1 expression in ZR-75-1 cells (Fig. 6C, upper panels). Moreover, down-regulation of E2-induced transcription by TAM was attenuated in ZR-75-1/vector, as compared to that in ZR-75-1/MUC1siRNA, cells (Fig. 6C, lower panel). In concert with these results, E2 stimulation of pS2 and cathepsin D expression at the mRNA (Fig. 6D) and protein levels (Fig. 6E) was attenuated by downregulation of MUC1 in both MCF-7 and ZR-75-1 cells. As a control, treatment with TAM for 3 to 48 h had no detectable effect on MUC1

expression in the MCF-7 and ZR-75-1 cells (Supplemental Figs. S6C and D). To further assess the effects of MUC1 on ERα-dependent transcription, MCF-7/CsiRNA and MCF-7/MUC1siRNA cells were transfected with ERE-tk-Luc and SRC-1 or GRIP1. Coactivation of ERE-tk-Luc by SRC-1 was enhanced to a greater extent in MCF-7/CsiRNA, as compared to MCF-7/MUC1siRNA, cells (Supplemental Figs. S7A and B). MUC1 also enhanced GRIP1-mediated coactivation of ERE-tk-Luc (Supplemental Figs. S7A and B). Similar results were obtained in ZR-75-1 cells, confirming that MUC1 increases coactivation of ERα-dependent transcription by SRC-1 and GRIP1 (supplemental Figs. S7C and D). These findings indicate that MUC1 i) increases occupancy of EREs by ERα/E2-coactivator complexes, ii) stimulates E2-mediated transcription and iii) antagonizes the inhibitory effects of TAM.

MUC1 enhances E2-dependent cell growth and survival. To assess the potential relevance of our results to the biology of breast cancer cells, we compared E2-mediated cell proliferation in MCF-7/CsiRNA and MCF-7/MUC1siRNA cells. E2 treatment was associated with an increase in MCF-7/CsiRNA cell growth (Fig. 7A). By contrast, E2 had little effect on growth of MCF-7/MUC1siRNA cells (Fig. 7A). E2 stimulation of ZR-75-1 cell growth was also attenuated by silencing MUC1 expression (Fig. 7B). To investigate the effects of silencing MUC1 on E2-dependent survival, we used a cell death ELISA detection system. Cell death of MCF-7/CsiRNA, but not MCF-7/MUC1siRNA, cells was decreased by E2 stimulation (Fig. 7C). E2-dependent decreases in ZR-75-1 cell death were also detectable in the presence, but not the silencing, of MUC1 expression (Fig. 7D). These findings indicate that MUC1 contributes to E2-dependent growth and survival of MCF-7 and ZR-75-1 cells.

KEY RESEARCH ACCOMPLISHMENTS

Our results demonstrate that MUC1 induces transformation by stabilizing the Wnt effector β-catenin (Cancer Research, in press). We have also found that MUC1 interacts with p53 and regulates p53-dependent gene transcription (Cancer Cell 7:167-178, 2005). In more

recent work, we show that the MUC1 C-terminal subunit associates with estrogen receptor α (ERα) and that this interaction is stimulated by 17β-estradiol (E2). MUC1 binds directly to the ERα DNA binding domain and stabilizes ERα by blocking its ubiquitination and degradation. Chromatin immunoprecipitation assays further demonstrate that MUC1 i) associates with ERα complexes on estrogen-responsive promoters, ii) enhances ERα promoter occupancy and iii) increases recruitment of p160 coactivators, SRC-1 and GRIP1. In concert with these results, we show that MUC1 stimulates ERα-mediated transcription and contributes to E2-mediated growth and survival of breast cancer cells. These findings provide the first evidence that MUC1 stabilizes ERα and that this oncoprotein is of importance to the activation of ERα function.

REPORTABLE OUTCOMES

1. Huang L, Chen D, Liu D, Yin L, Kharbanda S, Kufe D. MUC1 oncoprotein blocks GSK3β-mediated phosphorylation and degradation of β-catenin. Cancer Res. 2005; (in press).

2. Wei X, Xu H, Kufe D. Human MUC1 oncoprotein regulates p53-responsive gene transcription in the genotoxic stress response. Cancer Cell 2005; 7:167-178.

3. The results obtained regarding the interaction between MUC1 and ERα have been integrated into a manuscript that is being submitted for publication.

CONCLUSIONS

We conclude that MUC1 induces transformation and that the cytoplasmic domain is sufficient for this function by stabilizing β-catenin (Task 1). We also conclude that MUC1 associates with p53 and ERα and thereby contributes to the regulation of gene expression (Task 2). Work performed over the next year is being directed toward a more precise understanding of how MUC1 regulates gene expression and how these effects contribute to the induction of transformation.

REFERENCES

1. Kufe D, Inghirami G, Abe M, et al. Differential reactivity of a novel monoclonal antibody (DF3) with human malignant versus benign breast tumors. Hybridoma 1984;3:223-232.
2. Perey L, Hayes DF, Maimonis P, et al. Tumor selective reactivity of a monoclonal antibody prepared against a recombinant peptide derived from the DF3 human breast carcinoma-associated antigen. Cancer Res. 1992;52:2563-3568.
3. Swallow D, Gendler S, Griffiths B, et al. The human tumor associated epithelial mucins are coded by an expressed hypervariable gene locus PUM. Nature 1987;328:82-84.
4. Merlo G, Siddiqui J, Cropp C, et al. DF3 tumor-associated antigen gene is located in a region on chromosome 1q frequently altered in primary human breast cancer. Cancer Res. 1989;49:6966-6971.
5. Ligtenberg MJ, Kruijshaar L, Buijs F, et al. Cell-associated episialin is a complex containing two proteins derived from a common precursor. J. Biol. Chem. 1992;267:6171-6177.
6. Gendler S, Taylor-Papadimitriou J, Duhig T, Rothbard J, Burchell JA. A highly immunogenic region of a human polymorphic epithelial mucin expressed by carcinomas is made up of tandem repeats. J. Biol. Chem. 1988;263:12820-12823.
7. Siddiqui J, Abe M, Hayes D, et al. Isolation and sequencing of a cDNA coding for the human DF3 breast carcinoma-associated antigen. Proc. Natl. Acad. Sci. USA 1988;85:2320-2323.
8. Li Y, Chen W, Ren J, et al. DF3/MUC1 signaling in multiple myeloma cells is regulated by interleukin-7. Cancer Biol. Ther. 2003;2:187-193.
9. Li Y, Liu D, Chen D, Kharbanda S, Kufe D. Human DF3/MUC1 carcinoma-associated protein functions as an oncogene. Oncogene 2003;22:6107-6110.
10. Li Y, Yu W-H, Ren J, et al. Heregulin targets γ-catenin to the nucleolus by a mechanism dependent on the DF3/MUC1 protein. Mol. Cancer Res. 2003;1:765-775.
11. Wen Y, Caffrey T, Wheelock M, Johnson K, Hollingsworth M. Nuclear association of the

cytoplasmic tail of MUC1 and β-catenin. J. Biol. Chem. 2003;278:38029-38039.

12. Ren J, Agata N, Chen D, et al. Human MUC1 carcinoma-associated protein confers resistance to genotoxic anti-cancer agents. Cancer Cell 2004;5:163-175.

13. Yamamoto M, Bharti A, Li Y, Kufe D. Interaction of the DF3/MUC1 breast carcinoma-associated antigen and β-catenin in cell adhesion. J. Biol. Chem. 1997;272:12492-12494.

14. Li Y, Kufe D. The human DF3/MUC1 carcinoma-associated antigen signals nuclear localization of the catenin p120ctn. Biochem. Biophys. Res. Commun. 2001;281:440-443.

15. Wei X, Xu H, Kufe D. Human MUC1 oncoprotein regulates p53-responsive gene transcription in the genotoxic stress response. Cancer Cell 2005;7:167-178.

16. Li Y, Ren J, Yu W-H, et al. The EGF receptor regulates interaction of the human DF3/MUC1 carcinoma antigen with c-Src and β-catenin. J. Biol. Chem. 2001;276:35239-35242.

17. Li Y, Kuwahara H, Ren J, Wen G, Kufe D. The c-Src tyrosine kinase regulates signaling of the human DF3/MUC1 carcinoma-associated antigen with GSK3β and β-catenin. J. Biol. Chem. 2001;276:6061-6064.

18. Li Y, Bharti A, Chen D, Gong J, Kufe D. Interaction of glycogen synthase kinase 3β with the DF3/MUC1 carcinoma-associated antigen and β-catenin. Mol. Cell. Biol. 1998;18:7216-7224.

19. Schroeder J, Thompson M, Gardner M, Gendler S. Transgenic MUC1 interacts with epidermal growth factor receptor and correlates with mitogen-activated protein kinase activation in the mouse mammary gland. J. Biol. Chem. 2001;276:13057-13064.

20. Huang L, Ren J, Chen D, et al. MUC1 cytoplasmic domain coactivates Wnt target gene transcription and confers transformation. Cancer Biol. Ther. 2003;2:702-706.

21. Schroeder JA, Masri AA, Adriance MC, et al. MUC1 overexpression results in mammary gland tumorigenesis and prolonged alveolar differentiation. Oncogene 2004;23:5739-5747.

22. Huang L, Chen D, Liu D, et al. MUC1 oncoprotein blocks GSK3b-mediated phosphorylation and degradation of b-catenin. Cancer Res. (in press) 2005;

23. Ali S, Coombes RC. Endocrine-responsive breast cancer and strategies for combating resistance. Nat. Rev. Cancer 2002;2:101-112.

24. Lubahn DB, Moyer JS, Golding TS, et al. Alteration of reproductive function but not prenatal sexual development after insertional disruption of the mouse estrogen receptor gene. Proc. Natl. Acad. Sci. USA 1993;90:11162-11166.

25. Krege JH, Hodgin JB, Couse JF, et al. Generation and reproductive phenotypes of mice lacking estrogen receptor beta. Proc. Natl. Acad. Sci. USA 1998;95:15677-15682.

26. Kato S, Endoh H, Masuhiro Y, et al. Activation of the estrogen receptor through phosphorylation by mitogen-activated protein kinase. Science 1995;270:1491-1494.

27. Bourguet W, Ruff M, Chambon P, Gronemeyer H, Moras D. Crystal structure of the ligand-binding domain of the human nuclear receptor RXR-alpha. Nature 1995;375:377-382.

28. Chen H, Lin RJ, Schiltz RL, et al. Nuclear receptor coactivator ACTR is a novel histone acetyltransferase and forms a multimeric activation complex with P/CAF and CBP/p300. Cell 1997;90:569-580.

29. Onate SA, Tsai SY, Tsai MJ, O'Malley BW. Sequence and characterization of a coactivator for the steroid hormone receptor superfamily. Science 1995;270:1354-1357.

30. Cavailles V, Dauvois S, L'Horset F, et al. Nuclear factor RIP140 modulates transcriptional activation by the estrogen receptor. EMBO J. 1995;14:3741-3751.

31. Le Douarin B, Zechel C, Garnier JM, et al. The N-terminal part of TIF1, a putative mediator of the ligand-dependent activation function (AF-2) of nuclear receptors, is fused to B-raf in the oncogenic protein T18. EMBO J. 1995;14:2020-2033.

32. vom Baur E, Zechel C, Heery D, et al. Differential ligand-dependent interactions between the AF-2 activating domain of nuclear receptors and the putative transcriptional intermediary factors mSUG1 and TIF1. EMBO J. 1996;15:110-124.

33. Chakravarti D, LaMorte VJ, Nelson MC, et al. Role of CBP/p300 in nuclear receptor signalling. Nature 1996;383:99-103.

34. Shiau AK, Barstad D, Loria PM, et al. The structural basis of estrogen receptor/coactivator recognition and the antagonism of this interaction by tamoxifen. Cell 1998;95:927-937.

35. Ing NH, Beekman JM, Tsai SY, Tsai MJ, O'Malley BW. Members of the steroid hormone receptor superfamily interact with TFIIB (S300-II). J. Biol. Chem. 1992;267:17617-17623.

36. Jacq X, Brou C, Lutz Y, et al. Human TAFII30 is present in a distinct TFIID complex and is required for transcriptional activation by the estrogen receptor. Cell 1994;79:107-117.

37. Shang Y, Hu X, DiRenzo J, Lazar MA, Brown M. Cofactor dynamics and sufficiency in estrogen receptor-regulated transcription. Cell 2000;103:843-852.

38. Brzozowski AM, Pike AC, Dauter Z, et al. Molecular basis of agonism and antagonism in the oestrogen receptor. Nature 1997;389:753-758.

39. Lundy J, Thor A, Maenza R, et al. Monoclonal antibody DF3 correlates with tumor differentiation and hormone receptor status in breast patients. Breast Cancer Res. and Treat. 1985;5:269-276.

40. Nawaz Z, Lonard DM, Dennis AP, Smith CL, O'Malley BW. Proteasome-dependent degradation of the human estrogen receptor. Proc. Natl. Acad. Sci. USA 1999;96:1858-1862.

41. Lonard DM, Nawaz Z, Smith CL, O'Malley BW. The 26S proteasome is required for estrogen receptor-alpha and coactivator turnover and for efficient estrogen receptor-alpha transactivation. Mol. Cell 2000;5:939-948.

42. Reid G, Hubner MR, Metivier R, et al. Cyclic, proteasome-mediated turnover of unliganded and liganded ERalpha on responsive promoters is an integral feature of estrogen signaling. Mol. Cell 2003;11:695-707.

43. Dauvois S, Danielian PS, White R, Parker MG. Antiestrogen ICI 164,384 reduces cellular estrogen receptor content by increasing its turnover. Proc. Natl. Acad. Sci. USA 1992;89:4037-4041.

44. Giamarchi C, Solanas M, Chailleux C, et al. Chromatin structure of the regulatory regions

of pS2 and cathepsin D genes in hormone-dependent and -independent breast cancer cell lines. Oncogene 1999;18:533-541.

45. Augereau P, Miralles F, Cavailles V, et al. Characterization of the proximal estrogen-responsive element of human cathepsin D gene. Mol. Endocrinol. 1994;8:693-703.

46. Metivier R, Stark A, Flouriot G, et al. A dynamic structural model for estrogen receptor-alpha activation by ligands, emphasizing the role of interactions between distant A and E domains. Mol. Cell 2002;10:1019-1032.

47. Metivier R, Penot G, Hubner MR, et al. Estrogen receptor-alpha directs ordered, cyclical, and combinatorial recruitment of cofactors on a natural target promoter. Cell 2003;115:751-763.

48. Kim JH, Li H, Stallcup MR. CoCoA, a nuclear receptor coactivator which acts through an N-terminal activation domain of p160 coactivators. Mol. Cell 2003;12:1537-1549.

Figure Legends

Figure 1. MUC1 associates with ERα. A and B. Human MCF-7 (A) and ZR-75-1 (B) breast cancer cells were grown in phenol red-free medium supplemented with 10% charcoal-dextran-stripped FBS for 3 d. The cells were then left untreated or stimulated with 100 nM E2 for 3 h. Lysates were subjected to immunoprecipitation (IP) with anti-ERα or a control IgG. The immunoprecipitates were analyzed by immunoblotting (IB) with anti-MUC1-C and anti-ERα. **C and D.** COS-1 cells expressing Myc-MUC1-CD and ERα were stimulated with 100 nM E2 for 3 h. Anti-ERα (C) or anti-Myc (D) IPs were immunoblotted with anti-MUC1-C or anti-ERα. Lysates not subjected to IP were immunoblotted with anti-MUC1-C or anti-ERα (lower panels).

Figure 2. MUC1-CD binds directly to the ERα DNA binding domain. A. Schema depicting the structures of MUC1-CD and ERα. Also shown for MUC1-CD are the β-catenin binding motif (boxed) and the c-Src, GSK3β and PKCδ phosphorylation sites. H: hinge region. **B-E.** GST and GST-MUC1-CD(1-72) were bound to glutathione agarose and incubated with ^{35}S-labeled ERα or the indicated ERα deletion mutants (**B and C**). GST, GST-MUC1-CD(1-72) or the indicated GST-MUC1-CD deletion mutants bound to glutathione agarose were incubated ^{35}S-labeled ERα (**D**). GST-MUC1-CD was incubated with the indicated ^{35}S-labeled ERα proteins in the absence of ligand (Control) and in the presence of 100 nM E2 or 100 nM TAM (**E**). After washing, bound proteins were eluted and separated by SDS-PAGE. The gels were fixed, dried and subjected to phosphoimager analysis.

Figure 3. MUC1 stabilizes ERα. A. Lysates from the indicated MCF-7 (left) and ZR-75-1 (right) cells were immunoblotted with anti-ERα, anti-MUC1-C and anti-β-actin. WT: wild-type cells. **B and C.** The indicated MCF-7 (left) and ZR-75-1 (right) cells were treated with 5 μM MG132 for 24 h. Lysates were subjected to immunoblotting with the indicated antibodies (B). Anti-ERα immunoprecipitates were analyzed by immunoblotting with anti-Ub or anti-ERα (C). **D.** MCF-7/CsiRNA (■) and MCF-7/MUC1siRNA (□) cells were pulsed with

[^{35}S]-methionine, washed and incubated in the presence of 10 nM E2 for the indicated times. Lysates were immunoprecipitated with anti-ERα and the precipitates were analyzed by SDS-PAGE and autoradiography. A higher amount of MCF-7/MUC1siRNA cell lysate was used for immunoprecipitation to increase the ERα signals. Lysates not subjected to immunoprecipitation were immunoblotted with anti-β-actin. Intensity of the signals as determined by densitometric scanning is presented as the percentage of ERα remaining over time relative to control at 0 h.

Figure 4. MUC1 occupancy of estrogen-responsive gene promoters. A and B. Cells were grown in phenol red-free medium supplemented with 10% charcoal-dextran-stripped FBS for 3 d. Following treatment with 100 nM E2 for 1 h, cells were cross-linked with 1% formaldehyde and monitored by ChIP assays. Soluble chromatin from control and E2-treated MCF-7 or ZR-75-1 cells was immunoprecipitated with anti-MUC1-C or a control IgG. The final DNA extractions were amplified by PCR using pairs of primers that cover the indicated EREs or control regions (CRs) of the pS2 (A) and cathepsin D (B) gene promoters. **C and D.** In Re-ChIP experiments, soluble chromatin from the indicated cells was immunoprecipitated with anti-MUC1-C. The immune complexes were eluted by incubation with 10 mM DTT for 30 min at 37°C. After centrifugation, the supernatant was diluted 30 times with Re-ChIP buffer, followed by reprecipitation with anti-ERα and then detection of the indicated EREs or CRs in the pS2 (C) and cathepsin D (D) gene promoters. **E.** MCF-7 and ZR-75-1 cells were treated with 100 nM E2 for the indicated times. Soluble chromatin was immunoprecipitated with anti-MUC1-C or anti-ERα and analyzed for pS2 and cathepsin D ERE sequences.

Figure 5. MUC1 increases ERα occupancy of EREs and ERα-mediated transactivation. A. MCF-7/CsiRNA and MCF-7/MUC1siRNA-A cells were treated with 100 nM E2 for 1 h. Soluble chromatin was immunoprecipitated with anti-ERα and analyzed for pS2 and cathepsin D ERE sequences. **B.** MCF-7/MUC1siRNA-A (open bars) and MCF-7/CsiRNA (solid bars) cells were transfected with 500 ng ERE-tk-Luc (Chen et al., 1999), an internal control

LacZ expression plasmid (pCMV-LacZ) and the indicated amounts of an ERα expression vector. At 18 h after transfection, the cells were left untreated or stimulated with 100 nM E2 for 24 h. Luciferase activity was normalized to that obtained for LacZ and is presented as relative luciferase activity (mean±SD of 3 separate experiments) compared to that obtained with the E2-stimulated MCF-7/MUC1siRNA cells (open bar; normalized to 1) in lane 2. **C.** ZR-75-1/vector and ZR-75-1/MUC1siRNA cells were treated with 100 nM E2 for 1 h. Soluble chromatin was immunoprecipitated with anti-ERα and analyzed for pS2 and cathepsin D ERE sequences. **D.** ZR-75-1/MUC1siRNA (open bars) and ZR-75-1/vector (solid bars) cells were transfected with ERE-tk-Luc, pCMV-LacZ and ERα as indicated, stimulated with E2 and analyzed for luciferase activity as described for MCF-7 cells in B.

Figure 6. MUC1 enhances recruitment of p160 coactivators and stimulates ERα-mediated gene transcription. A. Soluble chromatin from the indicated cells was immunoprecipitated with anti-MUC1-C, released and reimmunoprecipitated with anti-SRC-1 or anti-GRIP1 and monitored for detection of the indicated EREs or CRs in the pS2 and cathepsin D promoters. **B and C.** Upper panels. Soluble chromatin from the indicated cells left untreated, treated with 100 nM E2 for 1 h or treated with 1 μM TAM for 1 h was immunoprecipitated with anti-SRC-1 or anti-GRIP1 and analyzed for pS2 (left) and cathepsin D (right) gene promoter sequences. Lower panels. MCF-7/MUC1siRNA-A (B; open bars), MCF-7/CsiRNA (B; solid bars), ZR-75-1/MUC1siRNA (C; open bars) and ZR-75-1/vector (C; solid bars) cells were transfected with 500 ng ERE-tk-Luc and 10 ng pCMV-LacZ. At 18 h after transfection, the cells were left untreated or stimulated with 100 nM E2 in the absence or presence of 1 μM TAM for 24 h. Relative luciferase activity is presented as the mean±SD of 3 separate experiments compared to that obtained with the E2-stimulated MUC1-negative cells (open bar; normalized to 1). **D and E.** The indicated cells were left untreated, treated with 100 nM E2 or 1 μM TAM for 24 h. RT-PCR was performed for analysis of pS2, cathepsin D and β-actin mRNA levels (D). Lysates were subjected to immunoblotting with the indicated antibodies (E).

Figure 7. A-D. MUC1 increases E2-dependent growth and survival. MCF-7/CsiRNA (solid bars), MCF-7/MUC1siRNA (open bars) (A and C), ZR-75-1/vector (solid bars) and ZR-75-1/MUC1siRNA (open bars) (B and D) were seeded at 10^4 cells/well in 24 well plates. After culturing in phenol red-free medium with 10% charcoal-dextran-stripped FBS for 2 d, the cells were maintained in medium without serum in the absence and presence of 100 nM E2 for 3 d. Cell growth was assessed by the Alamar Blue staining assay (A and B). The results are expressed as the percentage of cell growth (mean±SD of three separate experiments) as compared to that obtained for the MUC1-positive cells maintained in the absence of E2. Cell death was assessed using the cell death detection ELISA^{PLUS} system (C and D). The results are expressed as the percentage of dead cells (mean±SD of three separate experiments). **E.** Schema depicting the proposed interactions between MUC1 and ERα.

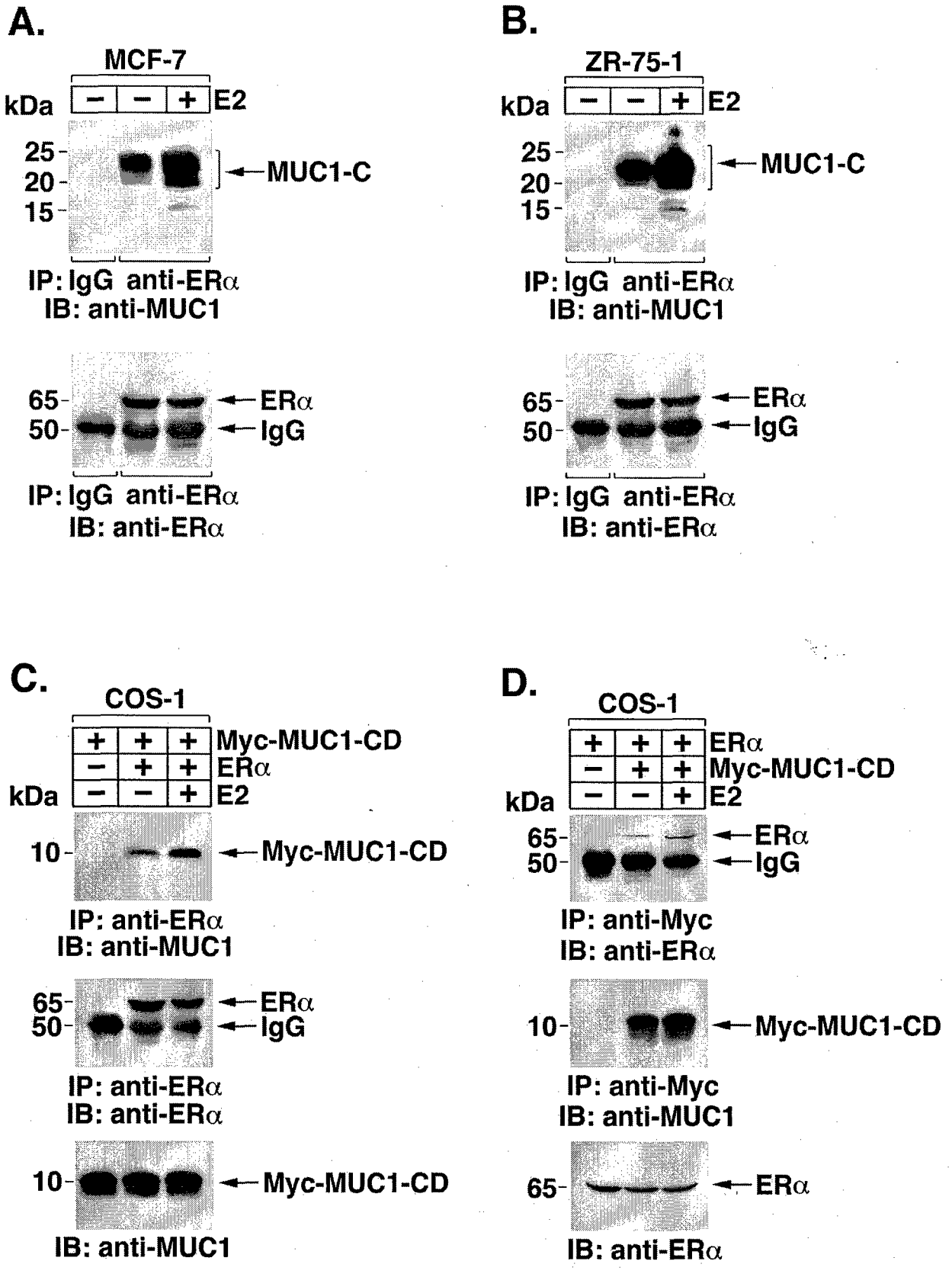
A.
MCF-7
kDa
– – + E2
25
20
15
MUC1-C
IP: IgG anti-ERα
IB: anti-MUC1
65
50
ERα
IgG
IP: IgG anti-ERα
IB: anti-ERα
B.
ZR-75-1
kDa
– – + E2
25
20
15
MUC1-C
IP: IgG anti-ERα
IB: anti-MUC1
65
50
ERα
IgG
IP: IgG anti-ERα
IB: anti-ERα
C.
COS-1
+ + + Myc-MUC1-CD
– + + ERα
kDa – – + E2
10
Myc-MUC1-CD
IP: anti-ERα
IB: anti-MUC1
65
50
ERα
IgG
IP: anti-ERα
IB: anti-ERα
10
Myc-MUC1-CD
IB: anti-MUC1
D.
COS-1
+ + + ERα
– + + Myc-MUC1-CD
kDa – – + E2
65
50
ERα
IgG
IP: anti-Myc
IB: anti-ERα
10
Myc-MUC1-CD
IP: anti-Myc
IB: anti-MUC1
65
ERα
IB: anti-ERα

Fig. 2AB

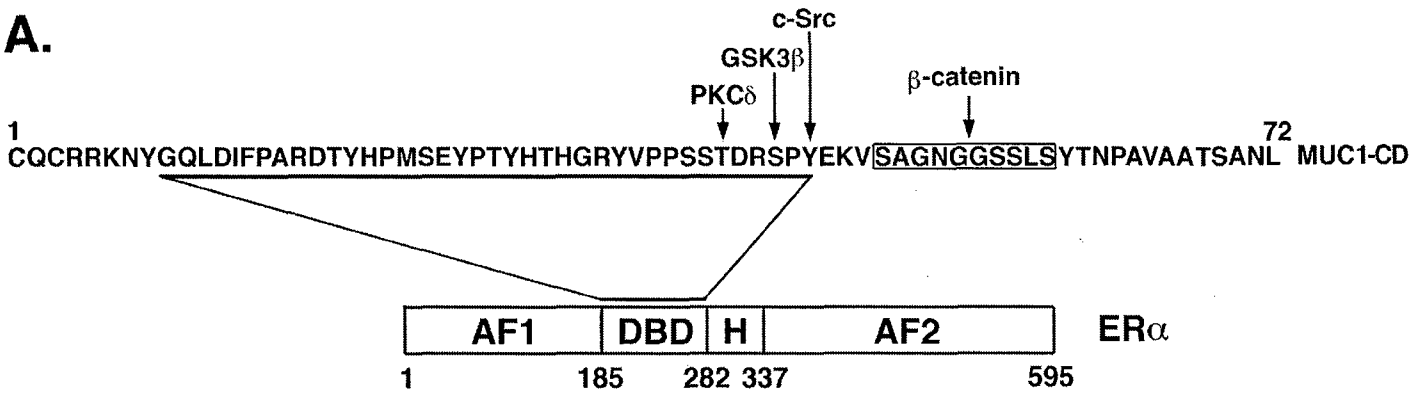
A.
c-Src
GSK3β
PKCδ
β-catenin
1
72
CQCRRKNYGQLDIFPARDTYHPMSEYPTYHTHGRYVPPSSTDRSPYEKVSAGNGGSSLSYTNPAVAATSANL
MUC1-CD
AF1
DBD
H
AF2
ERα
1
185
282
337
595

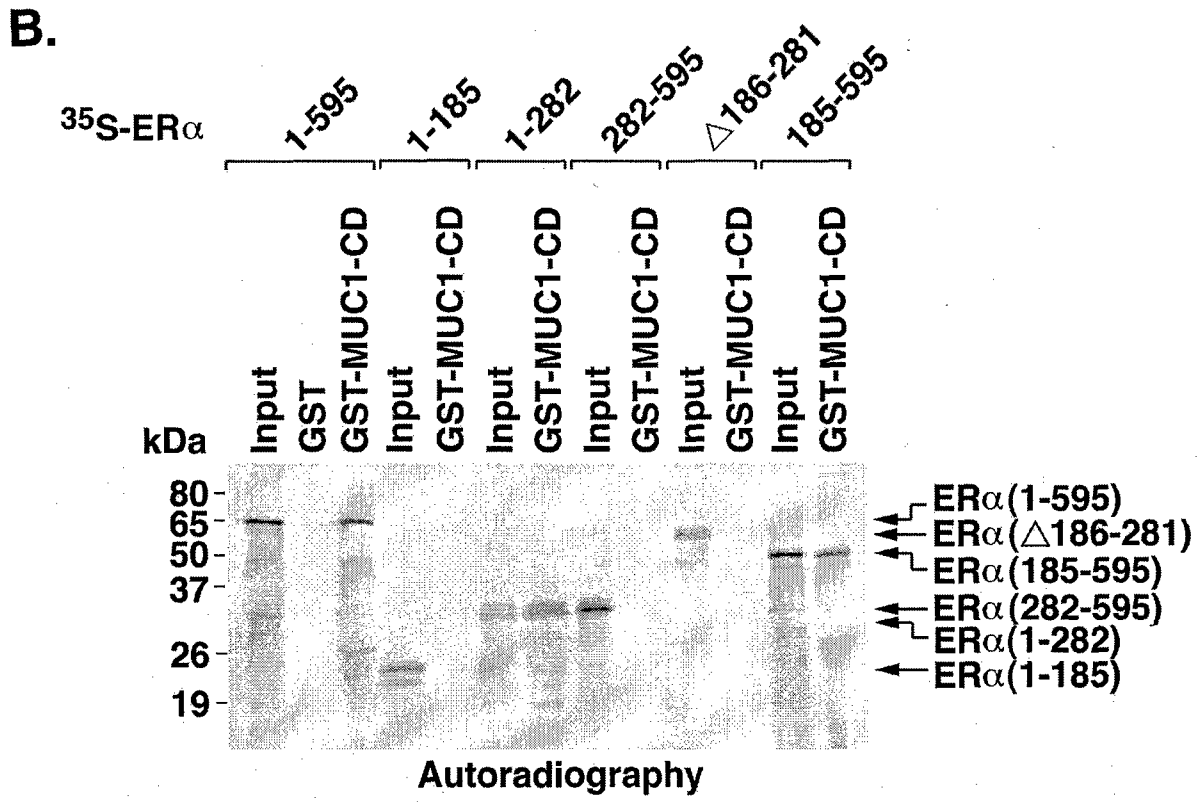
B.
35S-ERα
1-595
1-185
1-282
282-595
△186-281
185-595
Input
GST
GST-MUC1-CD
kDa
80
65
50
37
26
19
ERα(1-595)
ERα(△186-281)
ERα(185-595)
ERα(282-595)
ERα(1-282)
ERα(1-185)
Autoradiography

C.

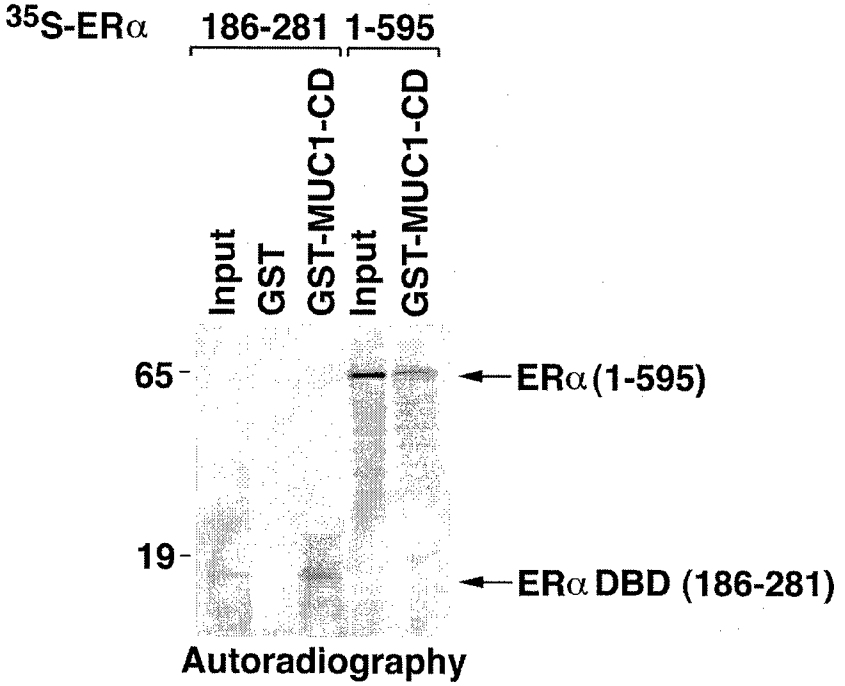
35S-ERα
186-281
1-595
Input
GST
GST-MUC1-CD
Input
GST-MUC1-CD
65
19
ERα(1-595)
ERα DBD (186-281)
Autoradiography

D.

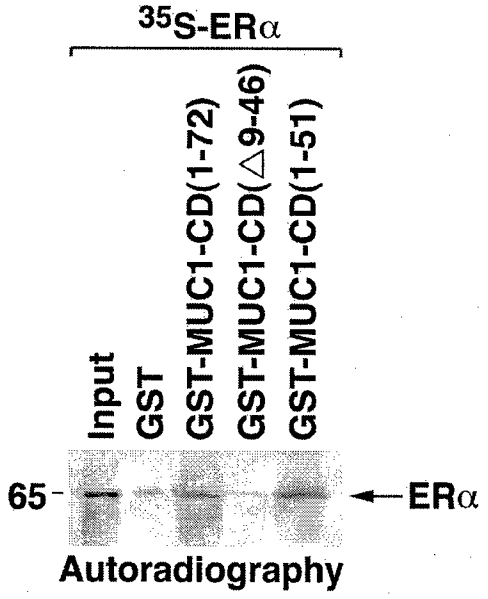
35S-ERα
Input
GST
GST-MUC1-CD(1-72)
GST-MUC1-CD(△9-46)
GST-MUC1-CD(1-51)
65
ERα
Autoradiography

E.

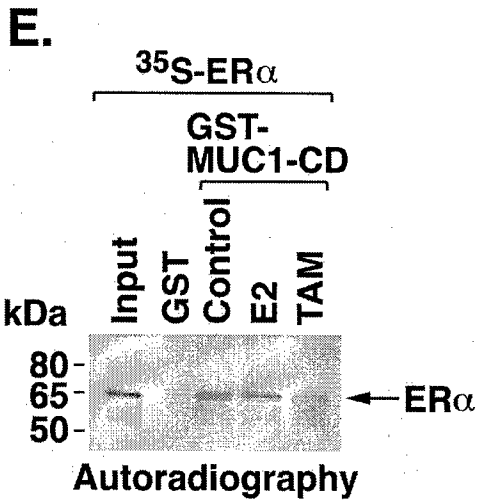
35S-ERα
GST-MUC1-CD
kDa
Input
GST
Control
E2
TAM
80
65
50
ERα
Autoradiography

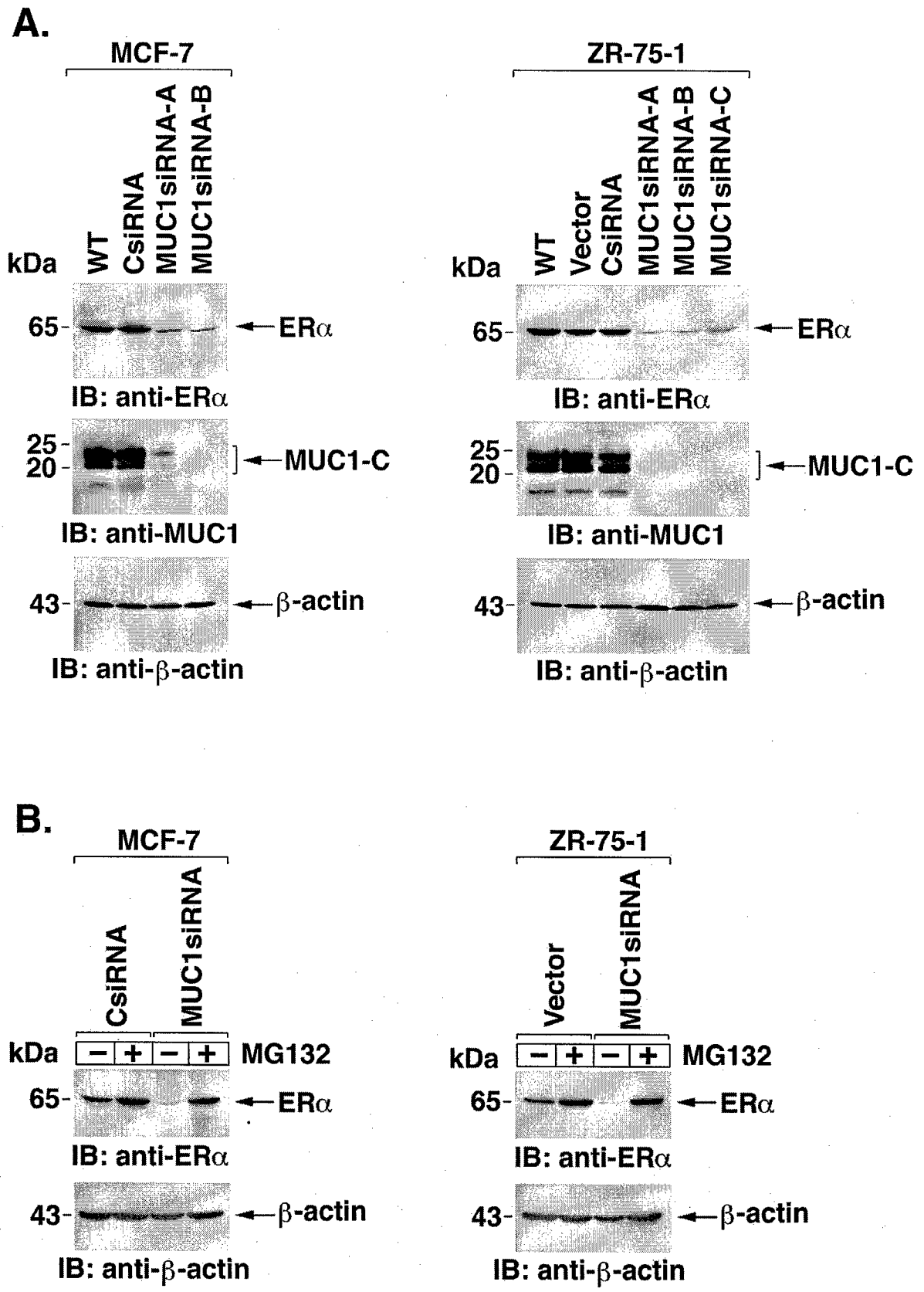
A.
MCF-7
WT
CsiRNA
MUC1siRNA-A
MUC1siRNA-B
kDa
65
ERα
IB: anti-ERα
25
20
MUC1-C
IB: anti-MUC1
43
β-actin
IB: anti-β-actin
ZR-75-1
WT
Vector
CsiRNA
MUC1siRNA-A
MUC1siRNA-B
MUC1siRNA-C
kDa
65
ERα
IB: anti-ERα
25
20
MUC1-C
IB: anti-MUC1
43
β-actin
IB: anti-β-actin
B.
MCF-7
CsiRNA
MUC1siRNA
kDa
− + − +
MG132
65
ERα
IB: anti-ERα
43
β-actin
IB: anti-β-actin
ZR-75-1
Vector
MUC1siRNA
kDa
− + − +
MG132
65
ERα
IB: anti-ERα
43
β-actin
IB: anti-β-actin

C.

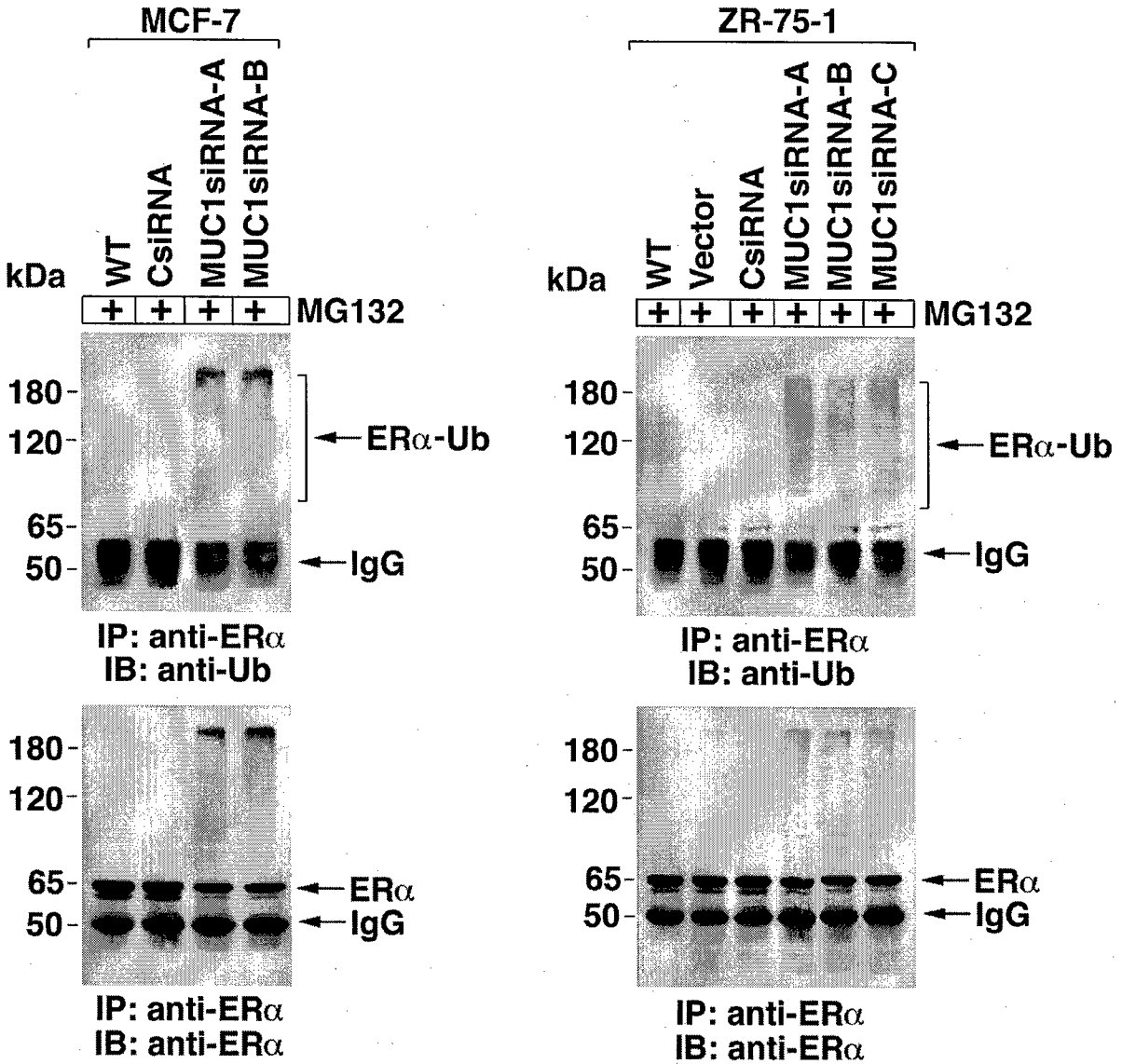
MCF-7
WT
CsiRNA
MUC1siRNA-A
MUC1siRNA-B
kDa
MG132
180
120
65
50
ERα-Ub
IgG
IP: anti-ERα
IB: anti-Ub
ERα
IP: anti-ERα
IB: anti-ERα
ZR-75-1
Vector
MUC1siRNA-C

Fig. 3D

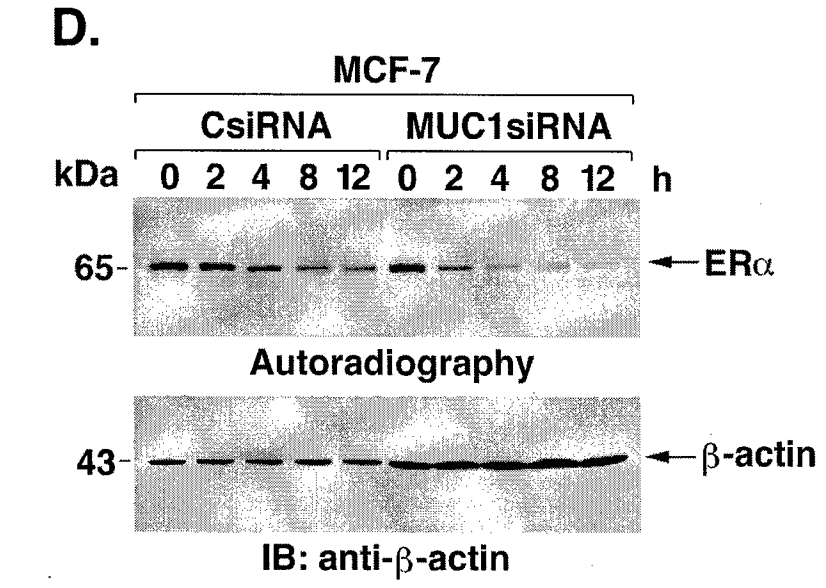
D.
MCF-7
CsiRNA
MUC1siRNA
kDa
0 2 4 8 12 0 2 4 8 12 h
65-
ERα
Autoradiography
43-
β-actin
IB: anti-β-actin

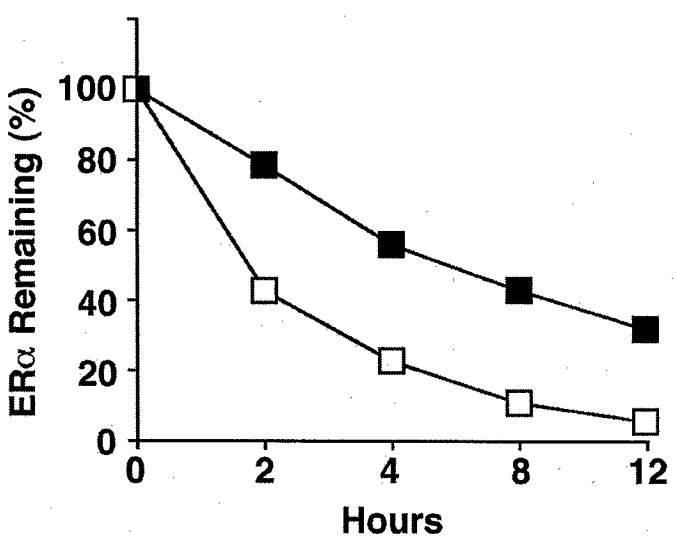
ERα Remaining (%)
100
80
60
40
20
0
0
2
4
8
12
Hours

Fig. 4AB

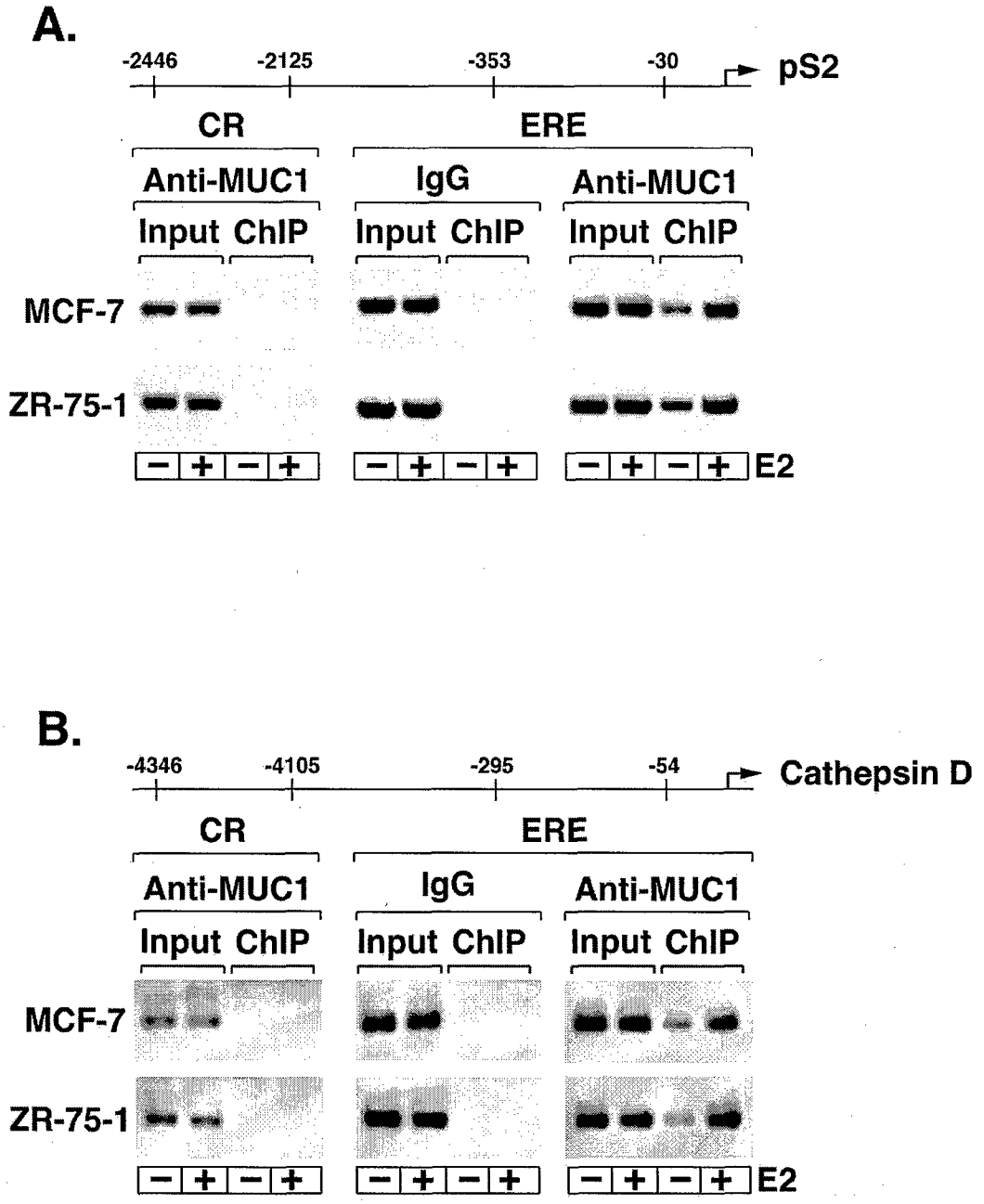
A.
-2446
-2125
-353
-30
pS2
CR
ERE
Anti-MUC1
IgG
Anti-MUC1
Input ChIP
Input ChIP
Input ChIP
MCF-7
ZR-75-1
− + − +
− + − +
− + − +
E2
B.
-4346
-4105
-295
-54
Cathepsin D
CR
ERE
Anti-MUC1
IgG
Anti-MUC1
Input ChIP
Input ChIP
Input ChIP
MCF-7
ZR-75-1
− + − +
− + − +
− + − +
E2

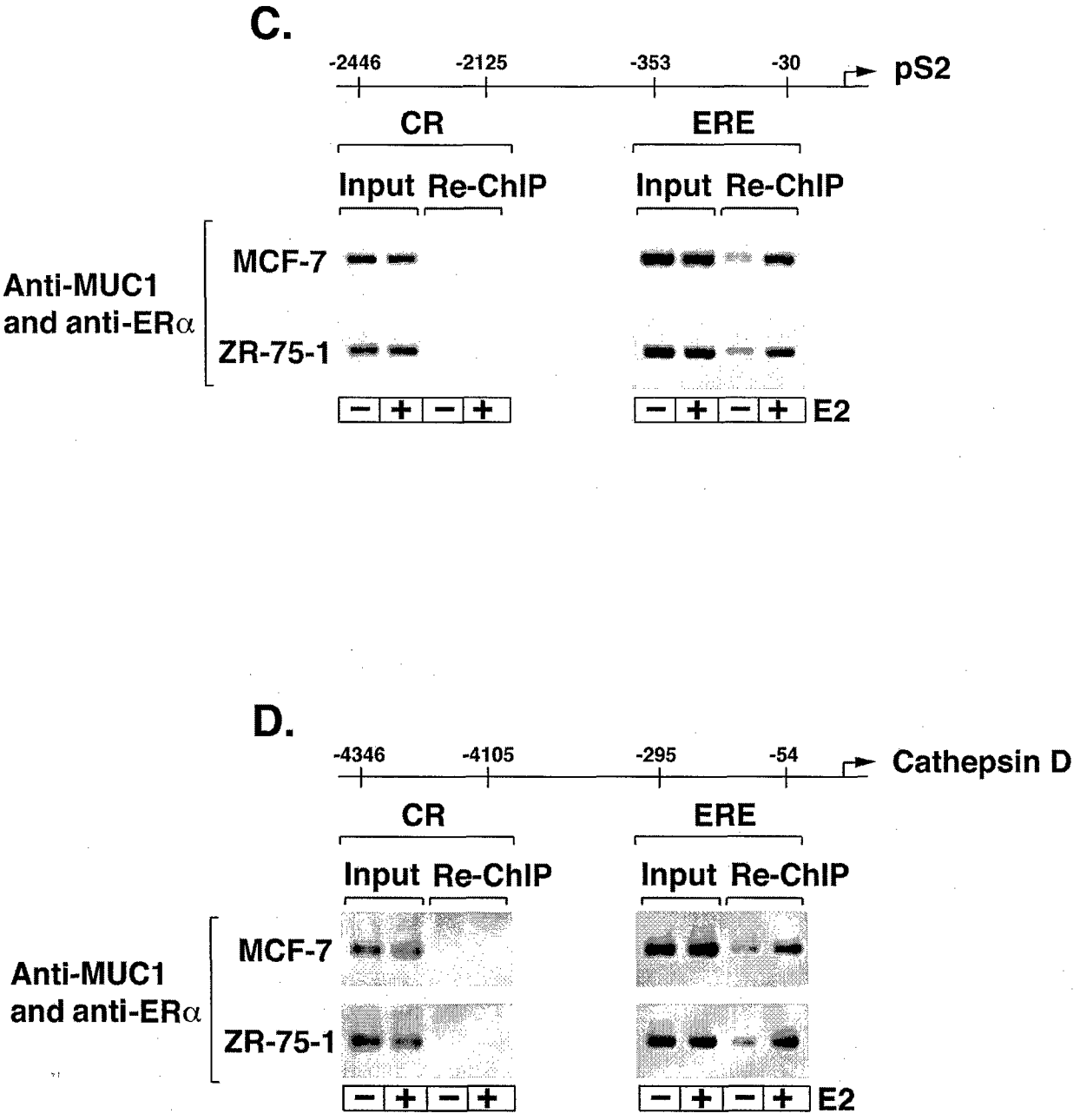
C.
-2446
-2125
-353
-30
pS2
CR
ERE
Input Re-ChIP
Input Re-ChIP
Anti-MUC1
and anti-ERα
MCF-7
ZR-75-1
− + − +
− + − +
E2
D.
-4346
-4105
-295
-54
Cathepsin D
CR
ERE
Input Re-ChIP
Input Re-ChIP
Anti-MUC1
and anti-ERα
MCF-7
ZR-75-1
− + − +
− + − +
E2

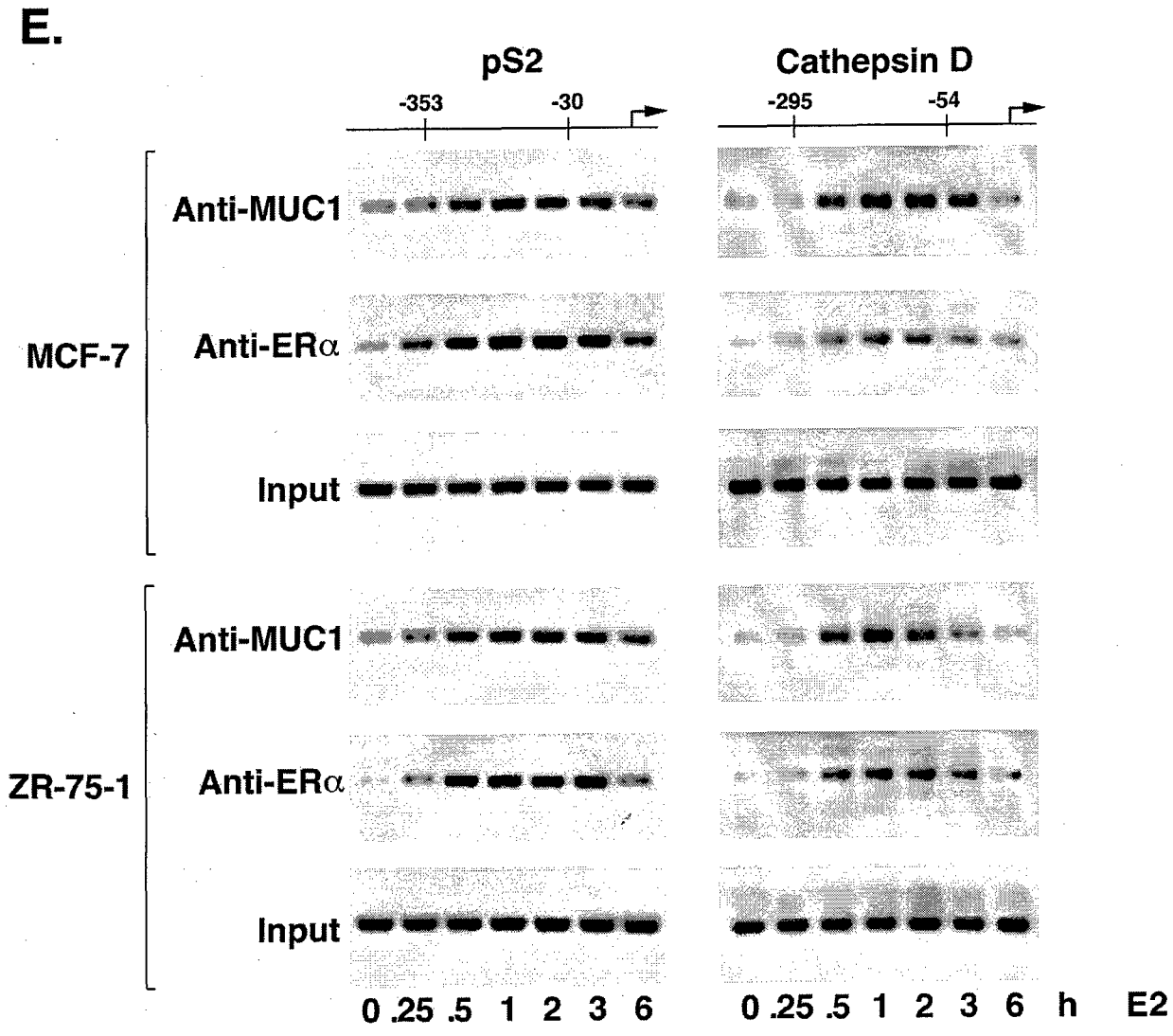
E.
pS2
-353
-30
Cathepsin D
-295
-54
MCF-7
Anti-MUC1
Anti-ERα
Input
ZR-75-1
Anti-MUC1
Anti-ERα
Input
0 .25 .5 1 2 3 6
0 .25 .5 1 2 3 6 h E2

Fig. 5AB

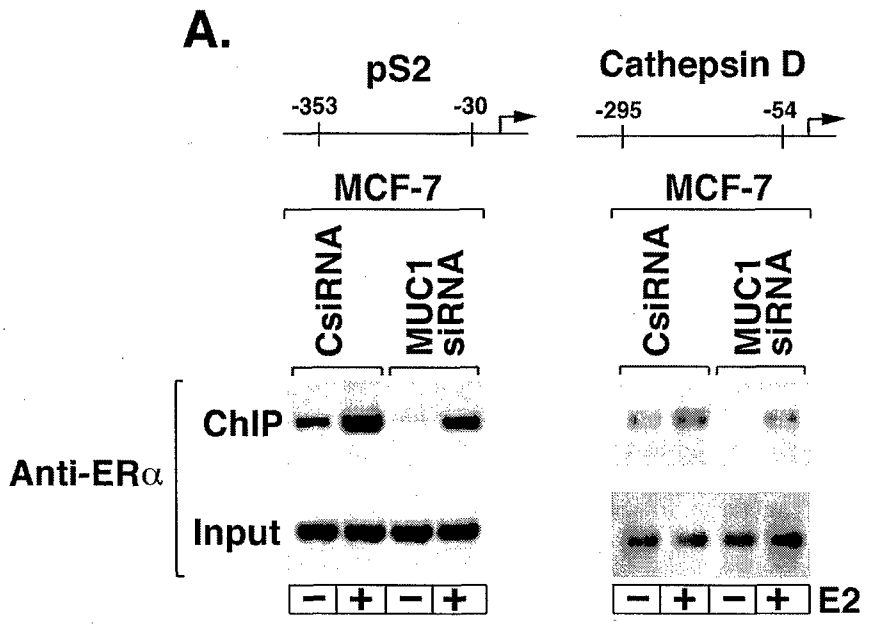
A.
pS2
-353
-30
Cathepsin D
-295
-54
MCF-7
MCF-7
CsiRNA
MUC1 siRNA
CsiRNA
MUC1 siRNA
Anti-ERα
ChIP
Input
− + − +
− + − + E2

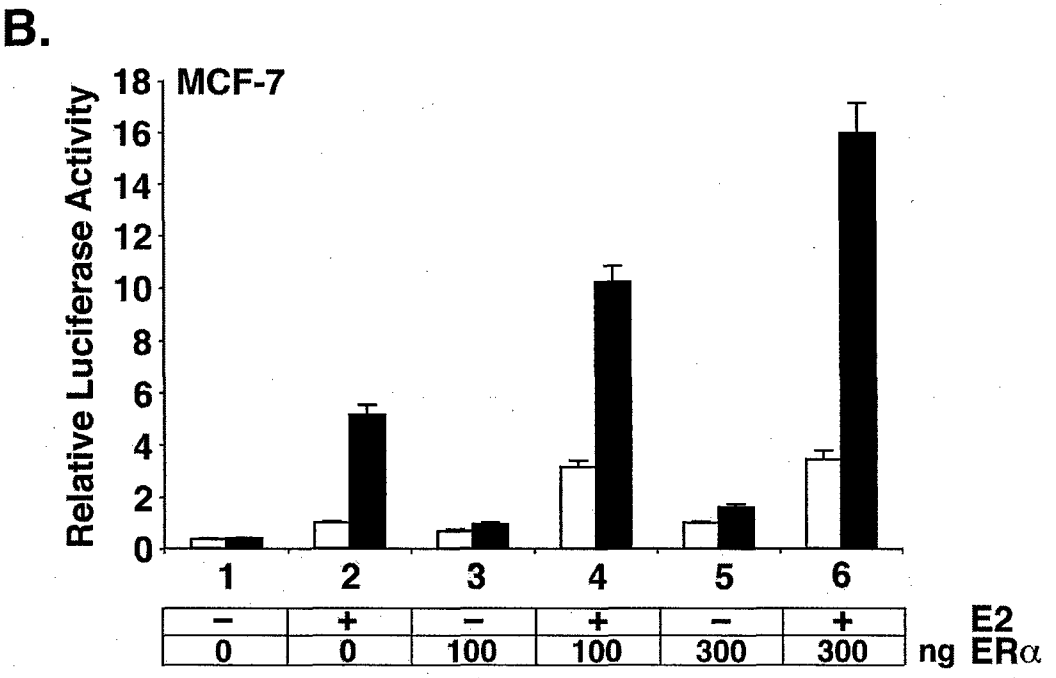
B.
MCF-7
Relative Luciferase Activity
18
16
14
12
10
8
6
4
2
0
1 2 3 4 5 6
− + − + − + E2
0 0 100 100 300 300 ng ERα

Fig. 5CD

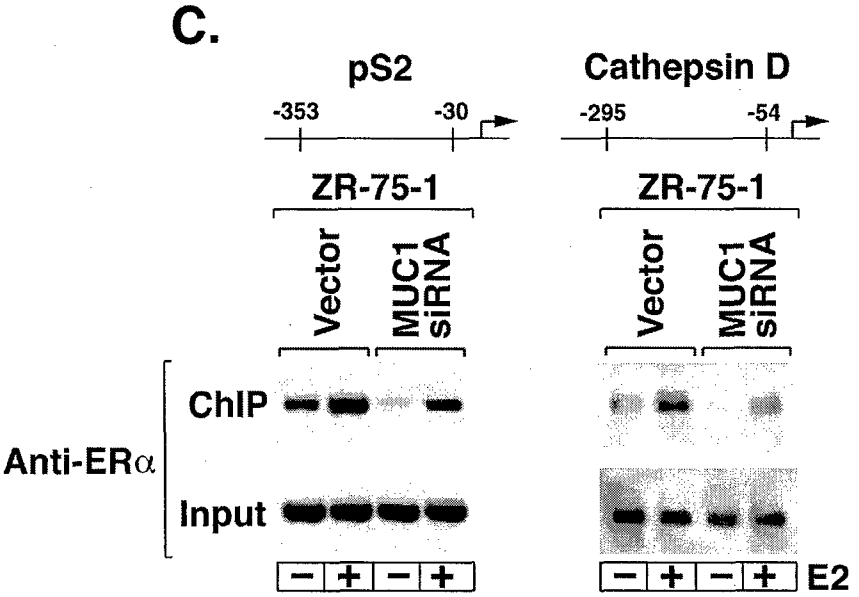
C.
pS2
Cathepsin D
-353
-30
-295
-54
ZR-75-1
ZR-75-1
Vector
MUC1 siRNA
Vector
MUC1 siRNA
Anti-ERα
ChIP
Input
− + − +
− + − +
E2

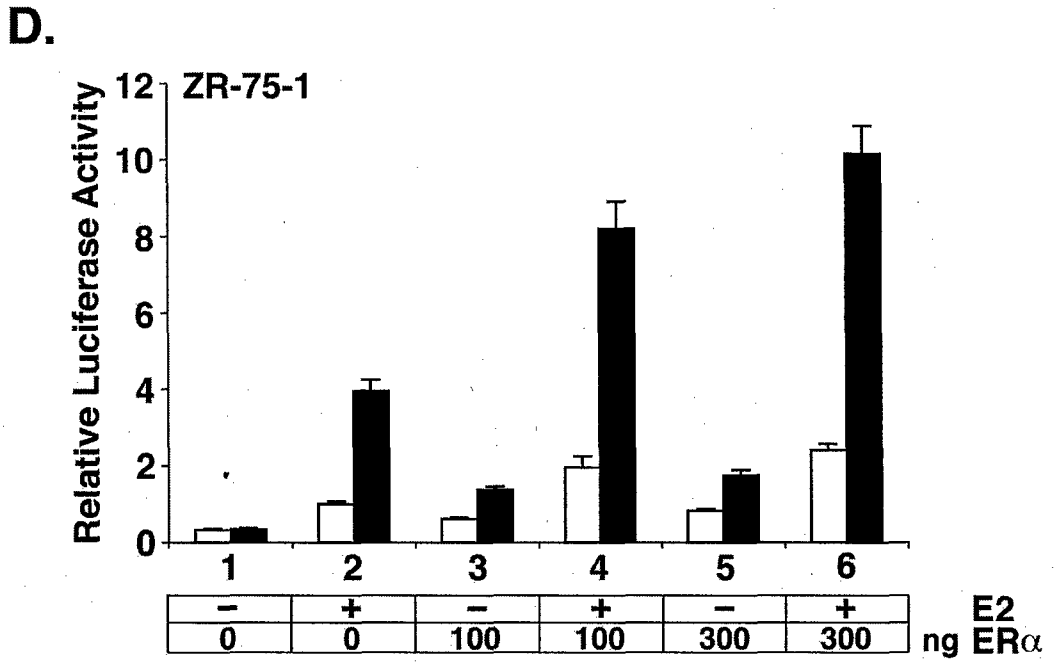
D.
ZR-75-1
Relative Luciferase Activity
0
2
4
6
8
10
12
1
2
3
4
5
6
− + − + − +
E2
0 0 100 100 300 300
ng ERα

Fig. 6A

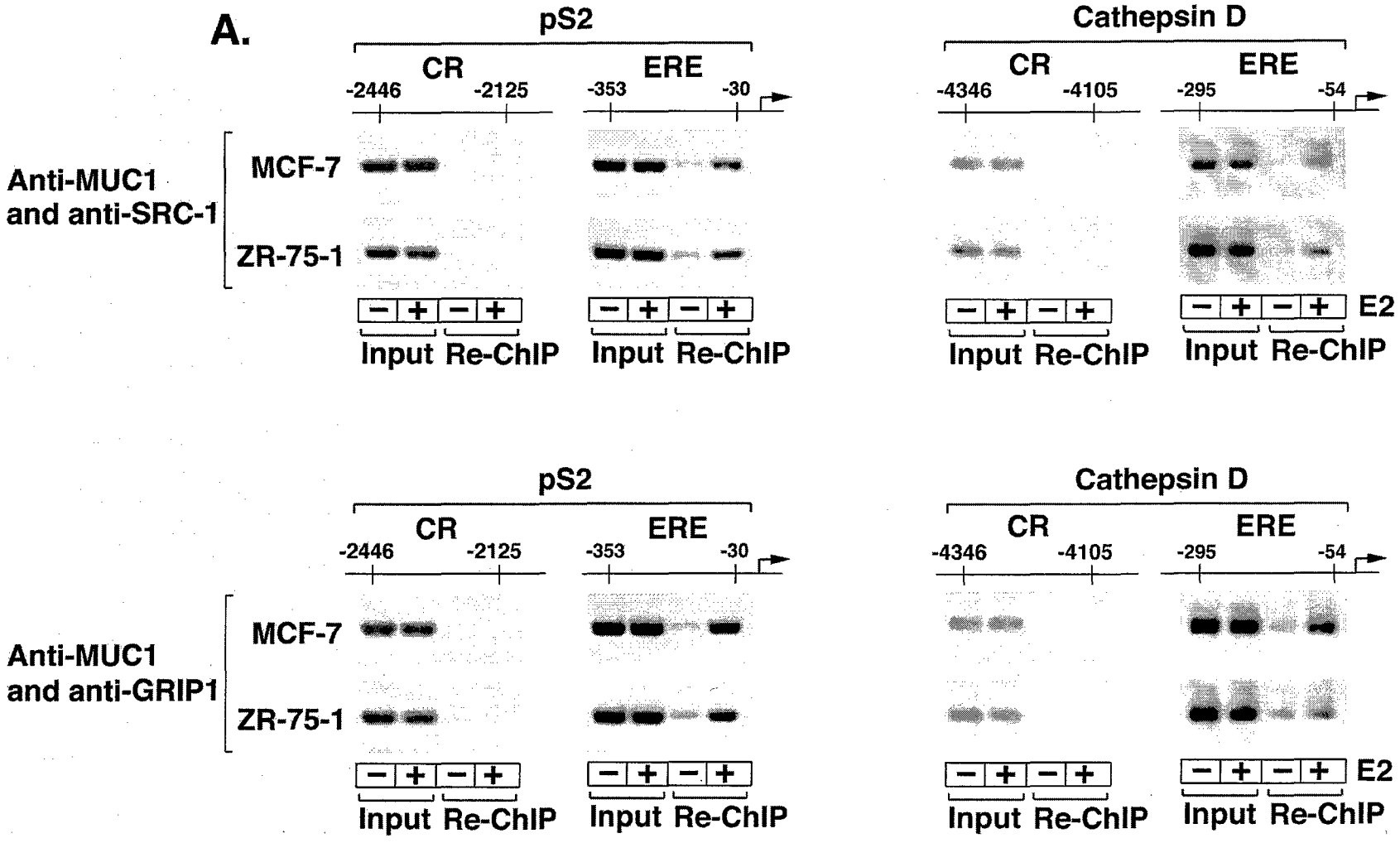
A.
pS2
CR
ERE
-2446
-2125
-353
-30
Cathepsin D
-4346
-4105
-295
-54
Anti-MUC1
and anti-SRC-1
MCF-7
ZR-75-1
E2
Input
Re-ChIP
Anti-MUC1
and anti-GRIP1

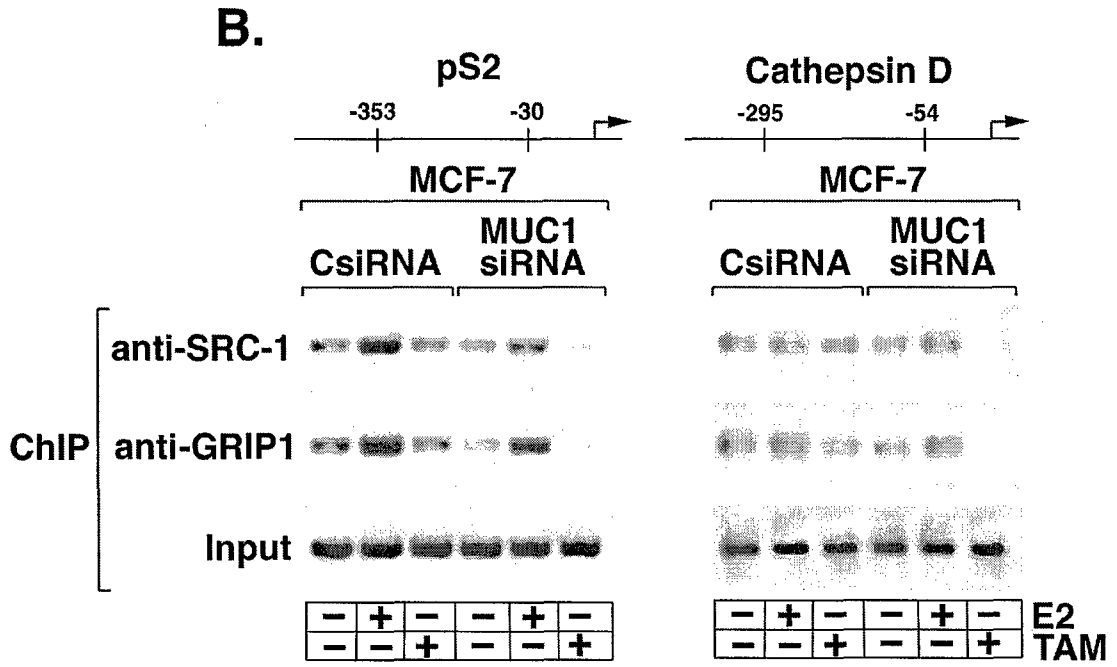
B.
pS2
-353
-30
Cathepsin D
-295
-54
MCF-7
MCF-7
CsiRNA
MUC1 siRNA
CsiRNA
MUC1 siRNA
ChIP
anti-SRC-1
anti-GRIP1
Input
E2
TAM

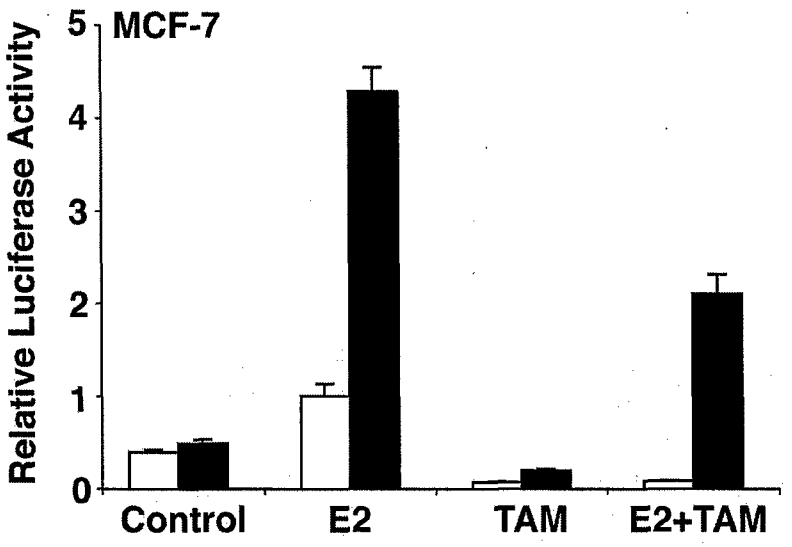
MCF-7
Relative Luciferase Activity
0
1
2
3
4
5
Control
E2
TAM
E2+TAM

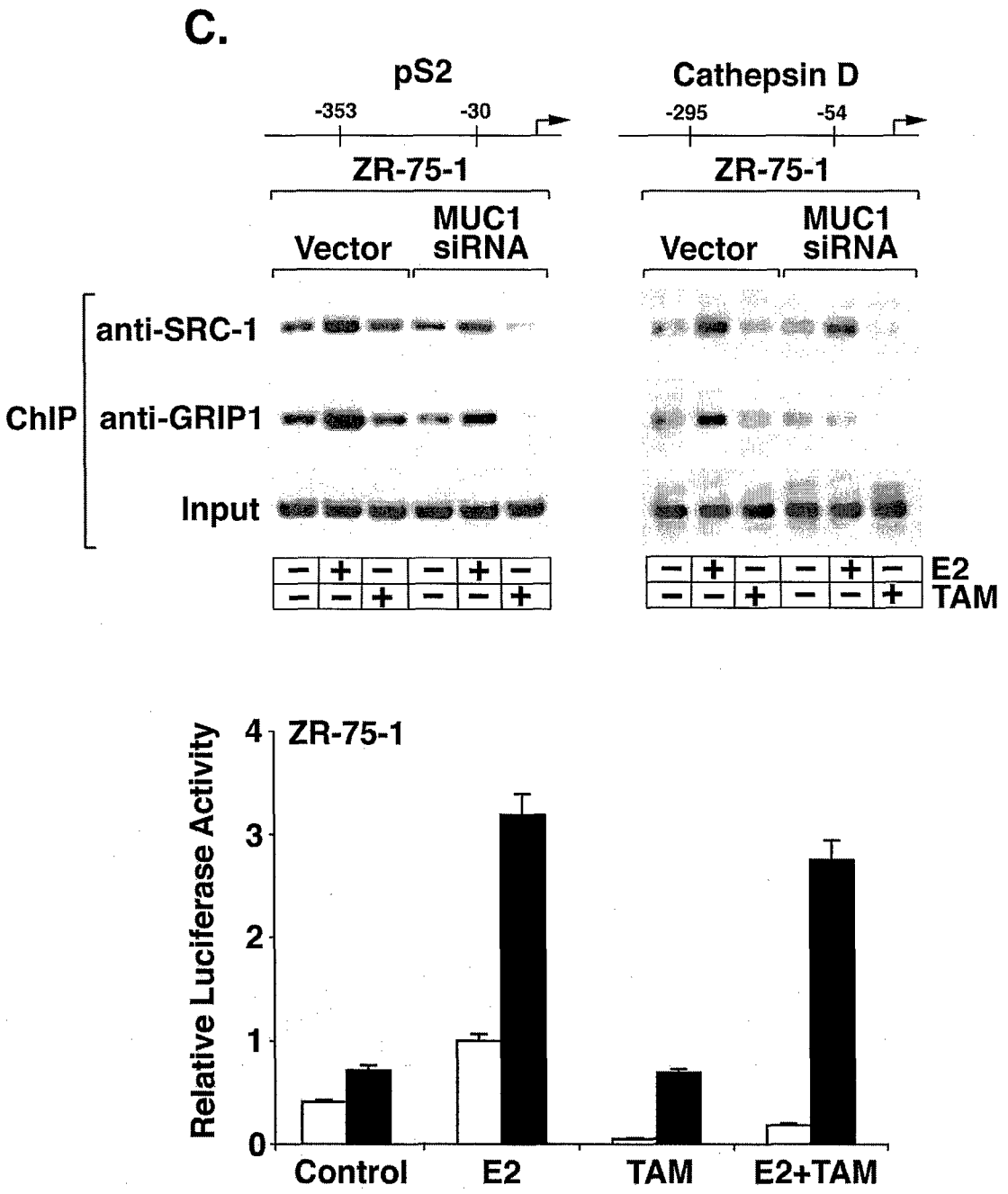
C.
pS2
-353
-30
Cathepsin D
-295
-54
ZR-75-1
ZR-75-1
Vector
MUC1 siRNA
Vector
MUC1 siRNA
ChIP
anti-SRC-1
anti-GRIP1
Input
E2
TAM
Relative Luciferase Activity
ZR-75-1
Control
E2
TAM
E2+TAM

Fig. 6DE

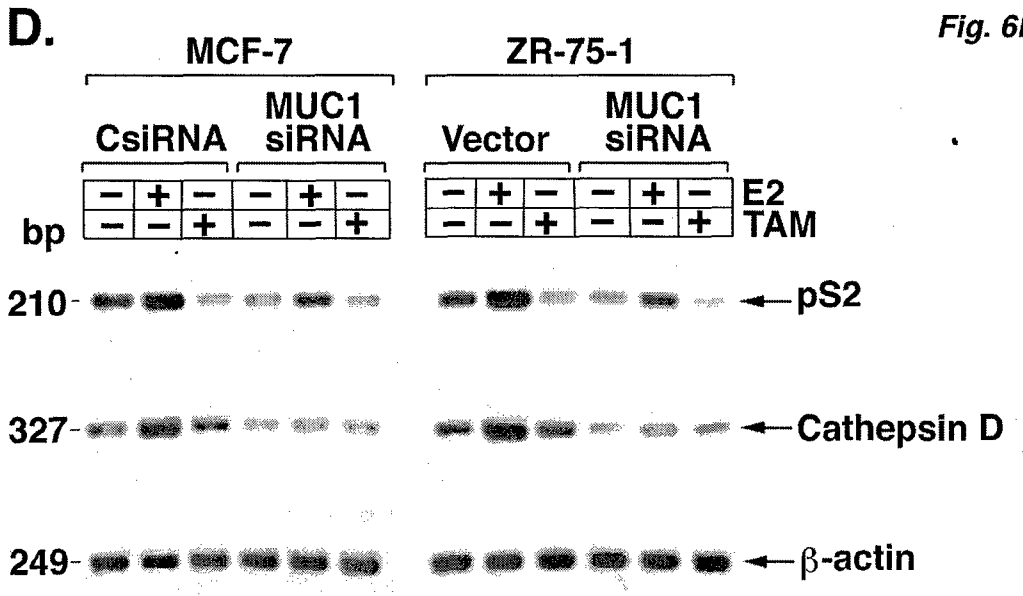
D.
MCF-7
ZR-75-1
CsiRNA
MUC1 siRNA
Vector
MUC1 siRNA
E2
TAM
bp
210
pS2
327
Cathepsin D
249
β-actin

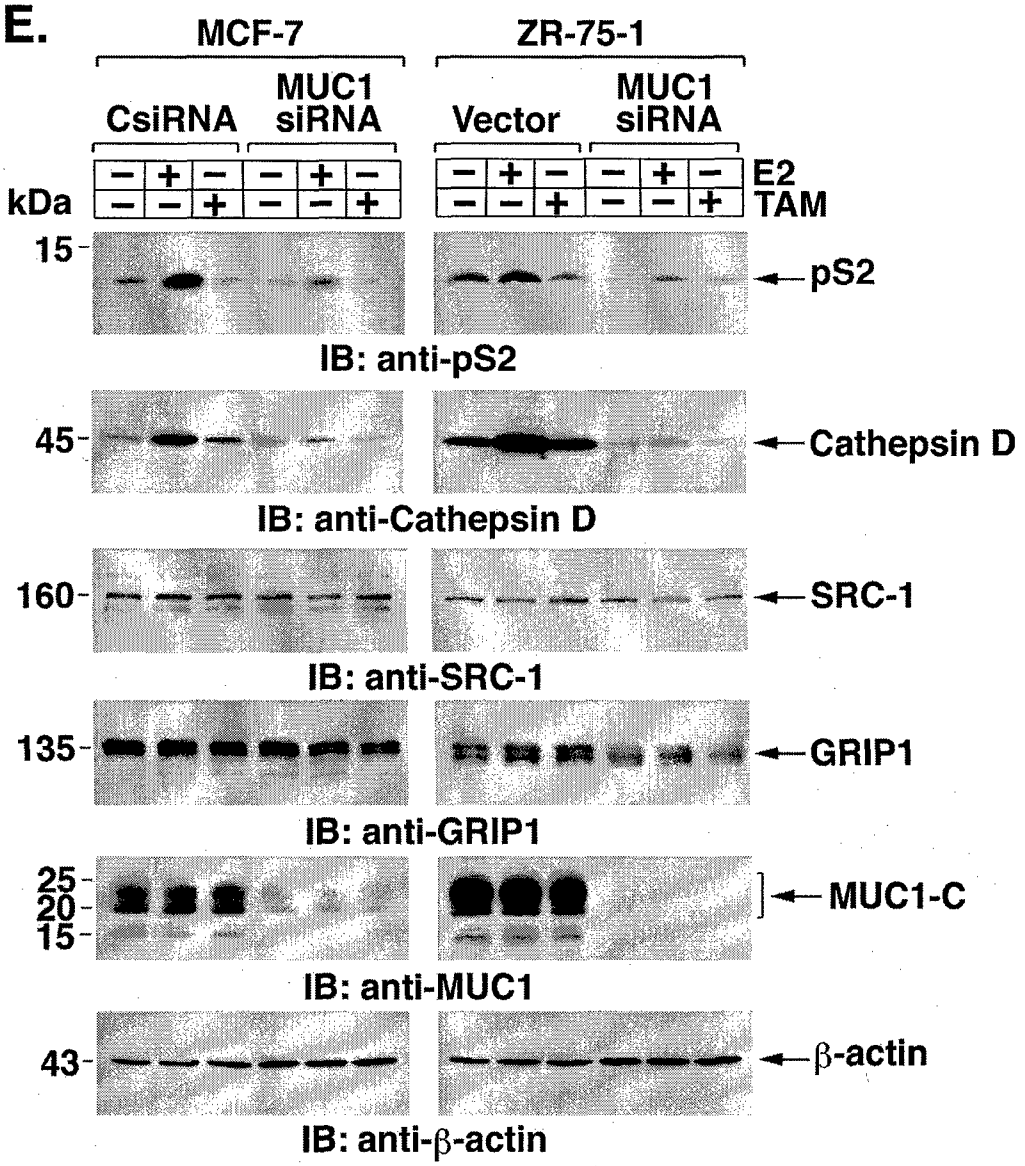
E.
MCF-7
ZR-75-1
CsiRNA
MUC1 siRNA
Vector
MUC1 siRNA
E2
TAM
kDa
15
pS2
IB: anti-pS2
45
Cathepsin D
IB: anti-Cathepsin D
160
SRC-1
IB: anti-SRC-1
135
GRIP1
IB: anti-GRIP1
25
20
15
MUC1-C
IB: anti-MUC1
43
β-actin
IB: anti-β-actin

Fig. 7ABCD

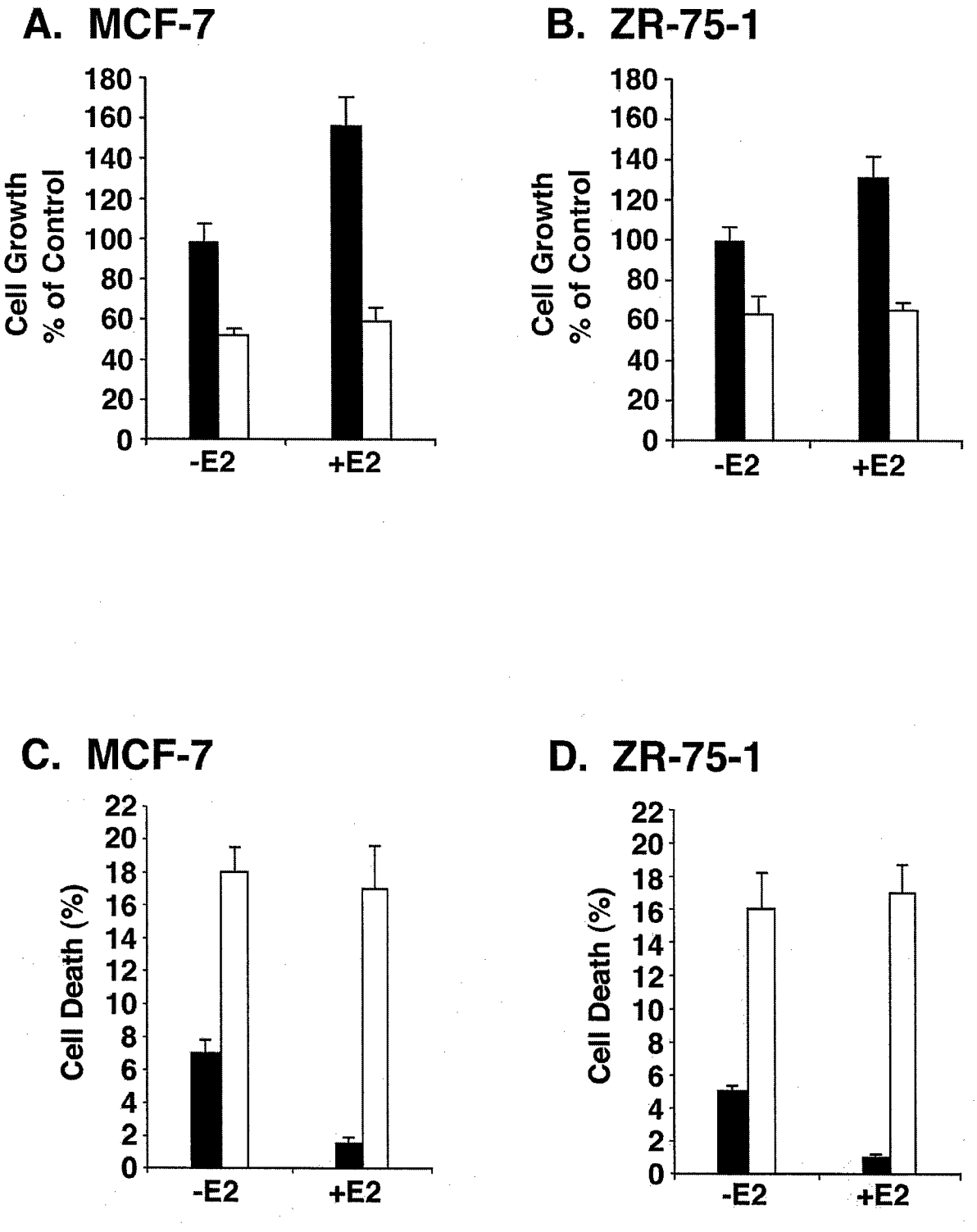
A. MCF-7
Cell Growth
% of Control
180
160
140
120
100
80
60
40
20
0
-E2
+E2
B. ZR-75-1
Cell Growth
% of Control
180
160
140
120
100
80
60
40
20
0
-E2
+E2
C. MCF-7
Cell Death (%)
22
20
18
16
14
12
10
8
6
4
2
0
-E2
+E2
D. ZR-75-1
Cell Death (%)
22
20
18
16
14
12
10
8
6
4
2
0
-E2
+E2

Fig. 7E

E.

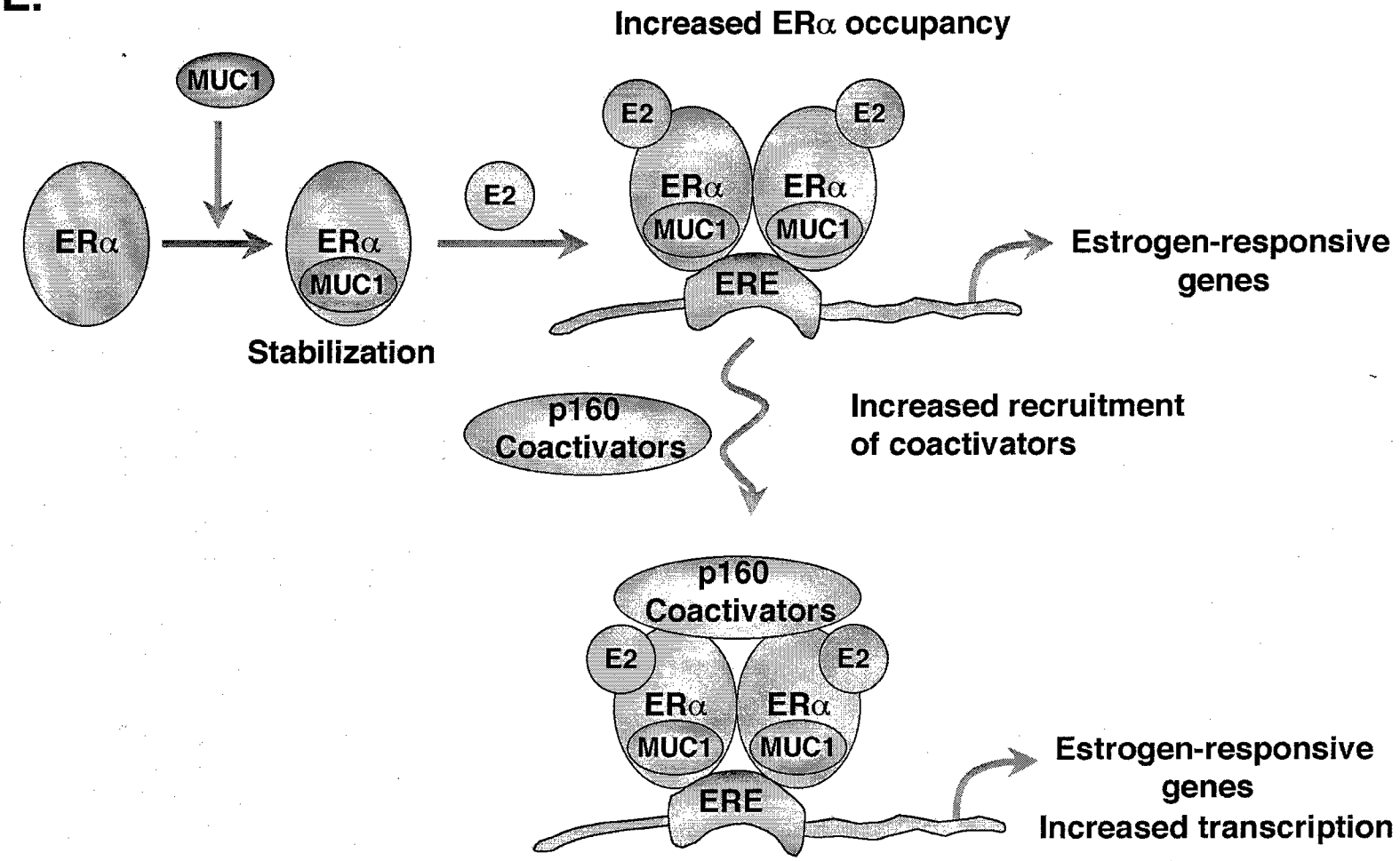
Increased ERα occupancy
MUC1
ERα
ERα
MUC1
Stabilization
E2
E2
E2
ERα
ERα
MUC1
MUC1
ERE
Estrogen-responsive genes
p160 Coactivators
Increased recruitment of coactivators
p160 Coactivators
E2
E2
ERα
ERα
MUC1
MUC1
ERE
Estrogen-responsive genes
Increased transcription

Supplemental Figure Legends

Figure S1. ERα associates with MUC1-C and not PCNA. A-F. MCF-7 (A and C) and ZR-75-1 (B and D) breast cancer cells were grown in phenol red-free medium supplemented with 10% charcoal-dextran-stripped FBS for 3 d. The cells were then left untreated or stimulated as indicated with 100 nM E2 for the indicated times (A and B) or for 3 h **(C-F).** Cells were also treated with 1 μM TAM for 3 h (C and D). Lysates were subjected to immunoprecipitation (IP) with anti-ERα (A-D), anti-PCNA (E and F) or a control IgG. The immunoprecipitates were analyzed by immunoblotting (IB) with the indicated antibodies. Whole cell lysates (WCL) not subjected to IP were immunoblotted with the indicated antibodies.

Figure S2. Silencing of MUC1 in MCF-7 and ZR-75-1 cells. A. MCF-7 cells were stably infected with retroviruses expressing a MUC1siRNA or a control siRNA (CsiRNA). Lysates were subjected to immunoblotting with anti-MUC1-C and anti-β-actin. **B.** Lysates from the indicated MCF-7 cells were immunoblotted with anti-ERα and anti-β-actin. Intensity of the signals was determined by densitometric scanning. The results (mean±SD of three separate experiments) represent relative ERα levels normalized to that in wild-type (WT) MCF-7 cells (assigned a value of 1). **C.** Lysates from the indicated MCF-7 and ZR-75-1 cells were immunoblotted with anti-ERα and anti-β-actin. **D.** ZR-75-1 cells were stably infected with an empty retrovirus (Vector) or one expressing MUC1siRNA. Lysates were subjected to immunoblotting with anti-MUC1-C and anti-β-actin. **E.** Lysates from the indicated ZR-75-1 cells were immunoblotted with anti-ERα and anti-β-actin. Intensity of the signals was determined by densitometric scanning. The results (mean±SD of three separate experiments) represent relative ERα levels normalized to that in wild-type (WT) ZR-75-1 cells (assigned a value of 1).

Figure S3. MUC1 attenuates ERα degradation. A and B. Semi-quantitative RT-PCR for ERα mRNA levels was performed on the indicated MCF-7 (A) and ZR-75-1 (B) cells. **C.** ZR-75-1/vector (▲) and ZR-75-1/MUC1siRNA (△) cells were pulsed with [^{35}S]-

methionine, washed and incubated in the presence of 10 nM E2 for the indicated times. Lysates were immunoprecipitated with anti-ERα and the precipitates were analyzed by SDS-PAGE and autoradiography. A higher amount of ZR-75-1/MUC1siRNA lysate was used for immunoprecipitation to increase the ERα signals. Lysates not subjected to immunoprecipitation were immunoblotted with anti-β-actin. Intensity of the signals as determined by densitometric scanning is presented as the percentage of ERα remaining over time relative to control at 0 h. **D.** The indicated ZR-75-1 cells were treated with 1 μM ICI for 6 and 12 h. Lysates were immunoblotted with anti-ERα and anti-β-actin.

Figure S4. Exogenous MUC1 in MDA-MB-231 cells occupies EREs by a mechanism dependent on ERα. A. MDA-MB-231 cells were transfected to stably express the empty vector or MUC1. Lysates from the transfectants and from ZR-75-1 cells were immunoblotted with the indicated antibodies. **B.** MDA-MB-231/vector and MDA-MB-231/MUC1 cells were transiently transfected to express ERα. Lysates from the transfectants were immunoblotted with the indicated antibodies. **C.** Soluble chromatin from the indicated cells was immunoprecipitated with anti-MUC1-C and analyzed for pS2 and cathepsin D promoter sequences.

Figure S5. Silencing MUC1 decreases MUC1 and ERα occupancy of EREs. A. MCF-7/CsiRNA and MCF-7/MUC1siRNA-A cells were treated with 100 nM E2 for 1 h. Soluble chromatin was immunoprecipitated with anti-MUC1 and analyzed for pS2 and cathepsin D ERE sequences. **B.** MCF-7/CsiRNA (solid bars) and MCF-7/MUC1siRNA (open bars) cells were treated with 100 nM E2 for 1 h. Soluble chromatin was immunoprecipitated with anti-ERα and analyzed for pS2 and cathepsin D occupancy. Intensity of the anti-ERα ChIP signals was determined by scanning densitometry. The results are expressed as relative ERα occupancy (mean±SD of three separate experiments) compared to that obtained in MUC1-positive cells without E2 stimulation (assigned a value of 1). **C.** ZR-75-1/vector and ZR-75-1/MUC1siRNA cells were treated with 100 nM E2 for 1 h. Soluble chromatin was

immunoprecipitated with anti-MUC1 and analyzed for pS2 and cathepsin D ERE sequences. **D.** ZR-75-1/vector (solid bars) and ZR-75-1/MUC1siRNA (open bars) cells were treated with 100 nM E2 for 1 h. Soluble chromatin was immunoprecipitated with anti-ERα and analyzed for pS2 and cathepsin D occupancy. Intensity of the anti-ERα ChIP signals was determined by scanning densitometry. The results are expressed as relative ERα occupancy (mean±SD of three separate experiments) compared to that obtained in MUC1-positive cells without E2 stimulation (assigned a value of 1).

Figure S6. MUC1 has little if any effect on ERα ligand binding affinity. **A.** Lysates from MCF-7/CsiRNA (▲,■) and MCF-7/MUC1siRNA (△,□) cells were incubated with the indicated concentrations of [^{3}H]-E2 in the absence (▲,△) and presence (■,□) of a 10-fold excess of TAM. The binding data shown are representative of three separate experiments. **B.** The binding data were transformed by the Scatchard method. **C and D.** MCF-7 (C) and ZR-75-1 (D) cells were treated with 1 μM TAM for the indicated times. Lysates were immunoblotted with anti-MUC1-C and anti-β-actin.

Figure S7. MUC1 potentiates coactivation of ERα-dependent transcription by SRC-1 and GRIP1. A-D. MCF-7/CsiRNA (solid bars), MCF-7/MUC1siRNA (open bars) (A) and ZR-75-1/vector (solid bars) and ZR-75-1/MUC1siRNA (open bars) (C) cells were transfected as indicated with 500 ng ERE-tk-Luc and 300 ng SRC-1 or 300 ng GRIP1. pCMV-LacZ was used an internal control. At 18 h after transfection, the cells were left untreated or stimulated with 100 nM E2 for 24 h. Relative luciferase activity is presented as the mean±SD of 3 separate experiments compared to that obtained with the E2-stimulated MUC1-negative cells (open bar; normalized to 1) in lane 2. Lysates from the transfected MCF-7 (B) and ZR-75-1 (D) cells were immunoblotted with the indicated antibodies.

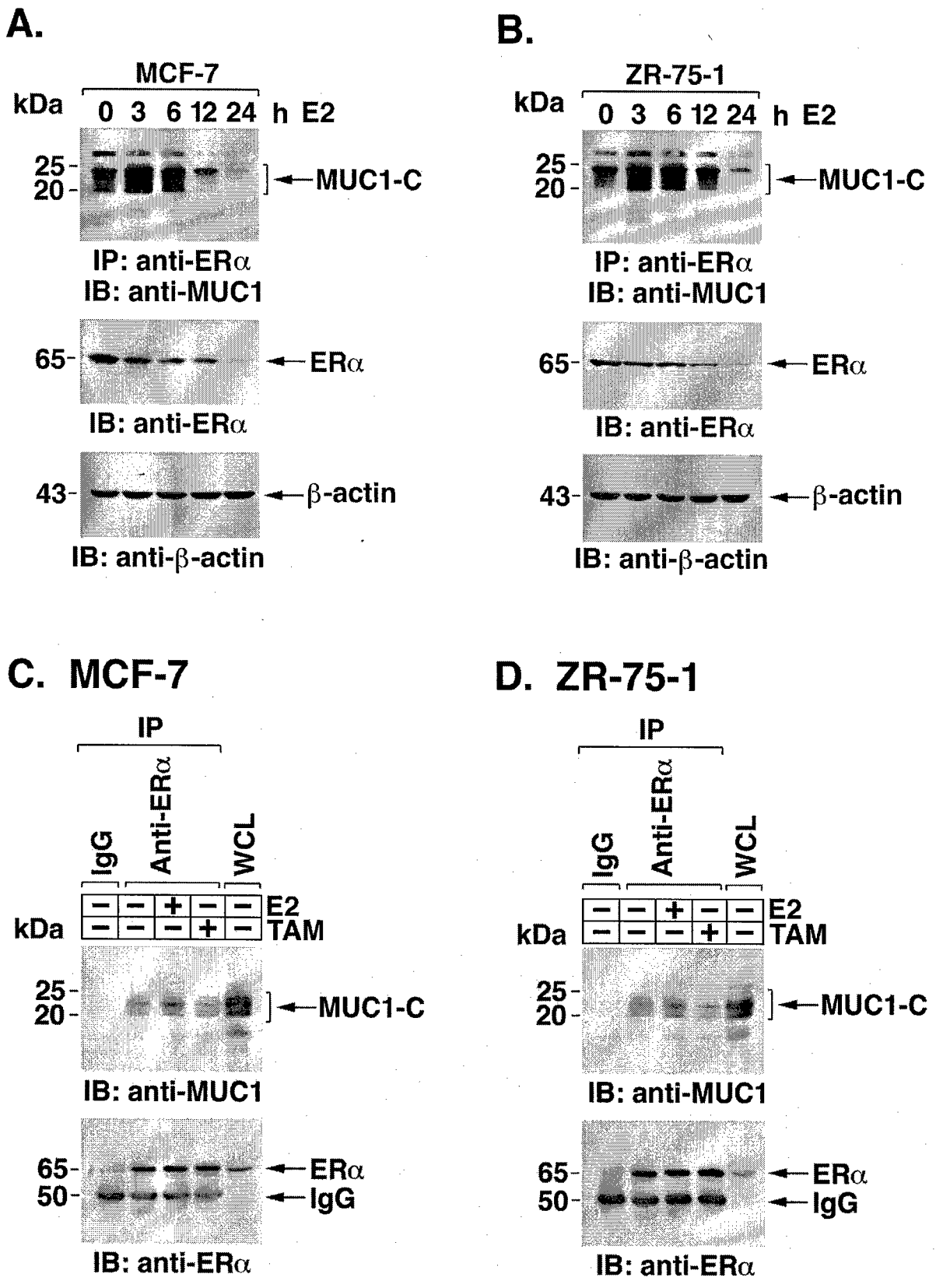
A.
MCF-7
kDa
0 3 6 12 24 h E2
25
20
MUC1-C
IP: anti-ERα
IB: anti-MUC1
65
ERα
IB: anti-ERα
43
β-actin
IB: anti-β-actin
B.
ZR-75-1
kDa
0 3 6 12 24 h E2
25
20
MUC1-C
IP: anti-ERα
IB: anti-MUC1
65
ERα
IB: anti-ERα
43
β-actin
IB: anti-β-actin
C. MCF-7
IP
IgG
Anti-ERα
WCL
kDa
E2
TAM
25
20
MUC1-C
IB: anti-MUC1
65
50
ERα
IgG
IB: anti-ERα
D. ZR-75-1
IP
IgG
Anti-ERα
WCL
kDa
E2
TAM
25
20
MUC1-C
IB: anti-MUC1
65
50
ERα
IgG
IB: anti-ERα

E. MCF-7

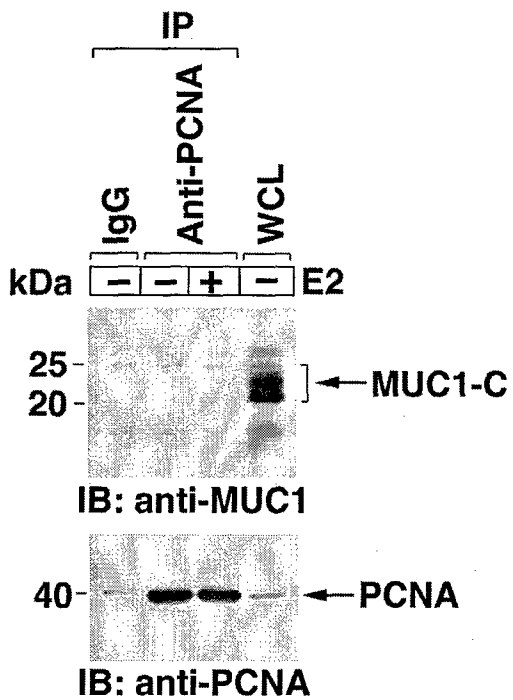

F. ZR-75-1

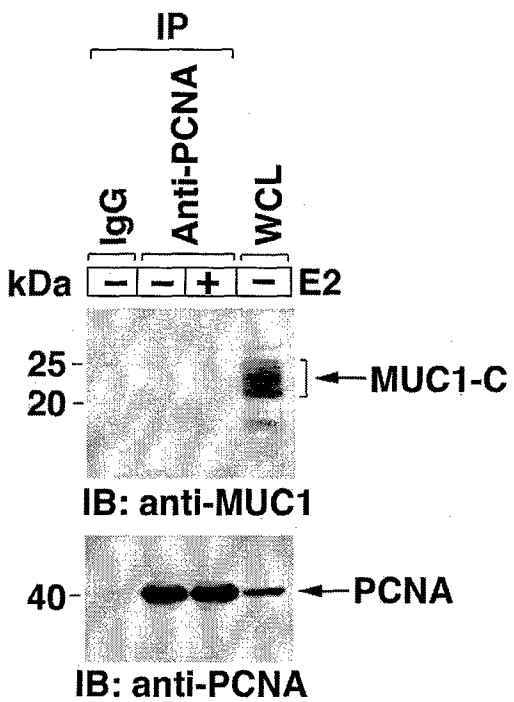

Fig. S2ABC

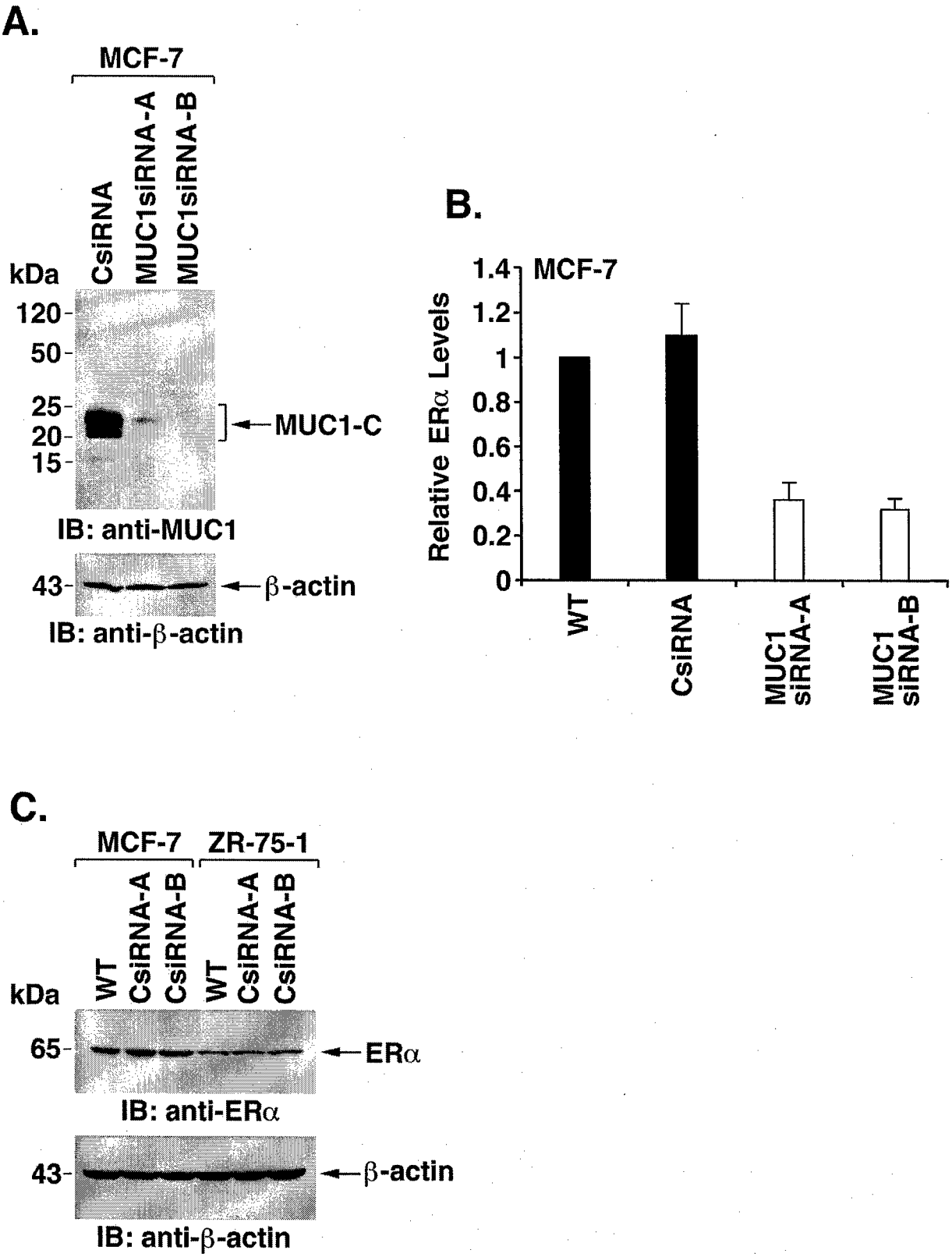
A.
MCF-7
CsiRNA
MUC1siRNA-A
MUC1siRNA-B
kDa
120
50
25
20
15
MUC1-C
IB: anti-MUC1
43
β-actin
IB: anti-β-actin
B.
MCF-7
Relative ERα Levels
1.4
1.2
1
0.8
0.6
0.4
0.2
0
WT
CsiRNA
MUC1 siRNA-A
MUC1 siRNA-B
C.
MCF-7
ZR-75-1
WT
CsiRNA-A
CsiRNA-B
WT
CsiRNA-A
CsiRNA-B
kDa
65
ERα
IB: anti-ERα
43
β-actin
IB: anti-β-actin

D.

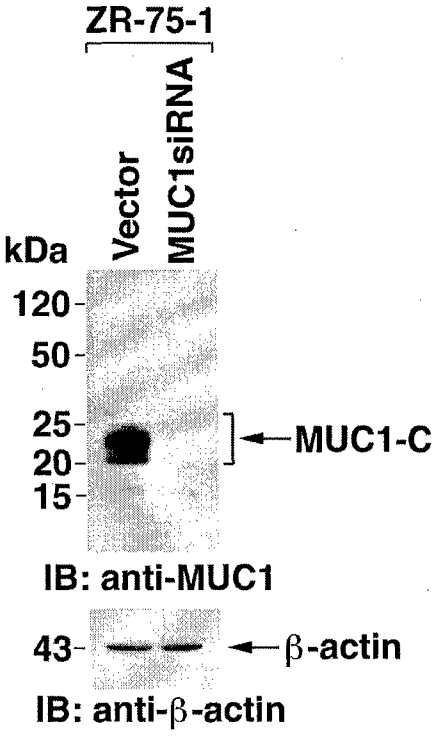
ZR-75-1
Vector
MUC1siRNA
kDa
120
50
25
20
15
MUC1-C
IB: anti-MUC1
43
β-actin
IB: anti-β-actin

E.

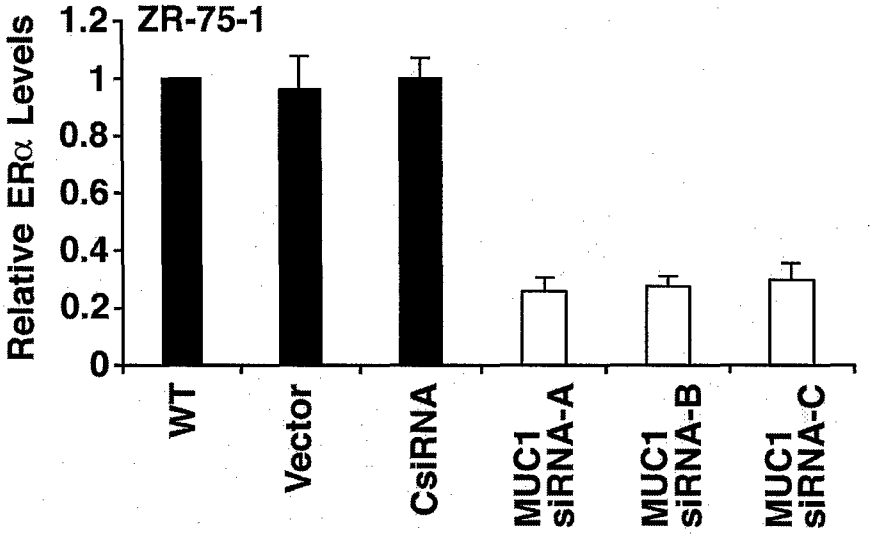
ZR-75-1
Relative ERα Levels
1.2
1
0.8
0.6
0.4
0.2
0
WT
Vector
CsiRNA
MUC1 siRNA-A
MUC1 siRNA-B
MUC1 siRNA-C

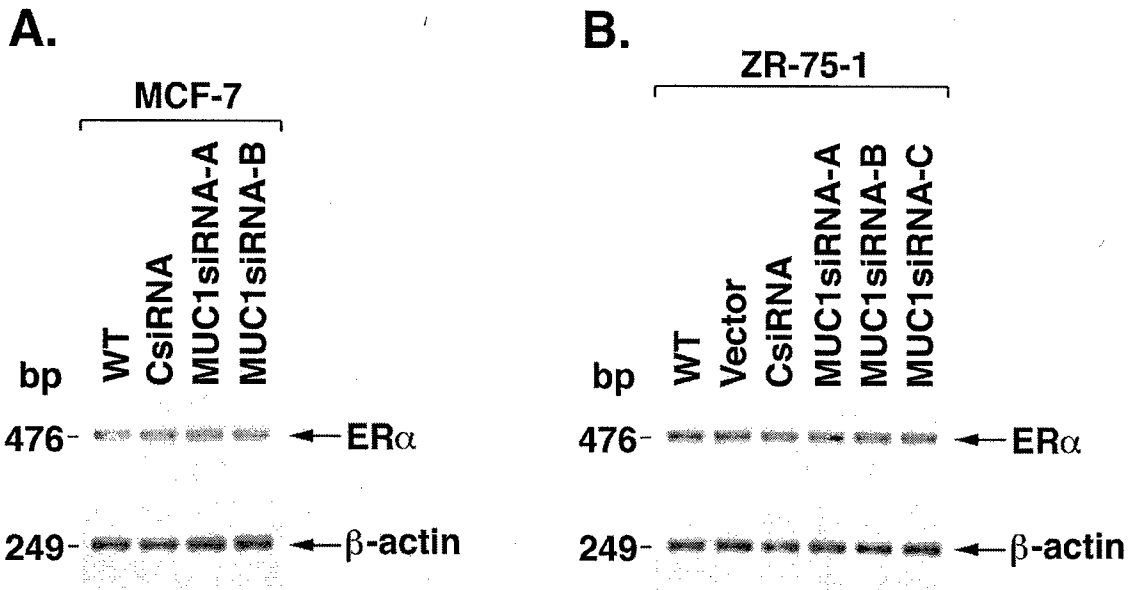
A.
MCF-7
WT
CsiRNA
MUC1siRNA-A
MUC1siRNA-B
bp
476-
ERα
249-
β-actin
B.
ZR-75-1
WT
Vector
CsiRNA
MUC1siRNA-A
MUC1siRNA-B
MUC1siRNA-C
bp
476-
ERα
249-
β-actin

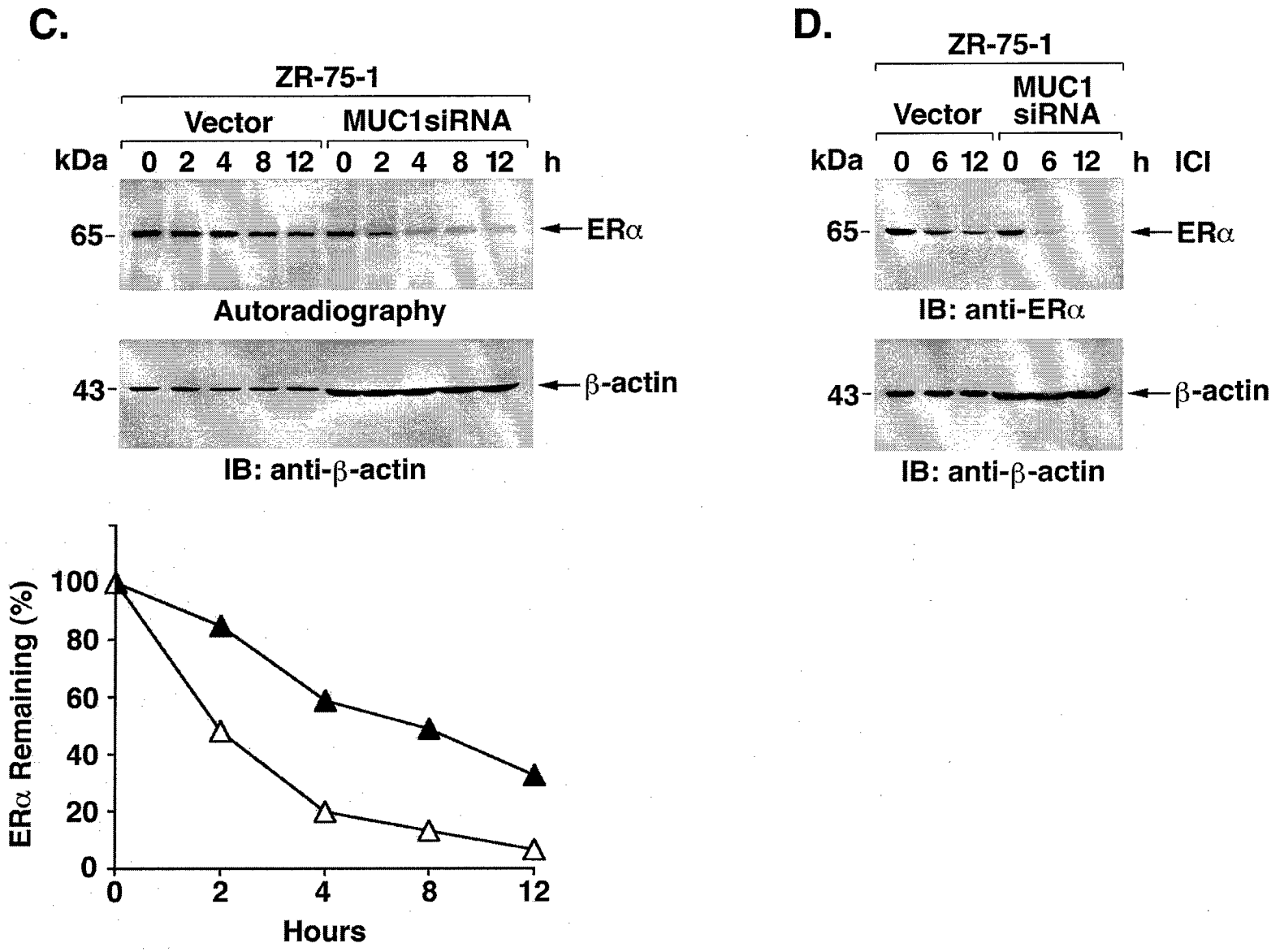
C.
ZR-75-1
Vector
MUC1siRNA
kDa
0 2 4 8 12 0 2 4 8 12 h
65-
ERα
Autoradiography
43-
β-actin
IB: anti-β-actin
ERα Remaining (%)
100
80
60
40
20
0
0 2 4 8 12
Hours
D.
ZR-75-1
Vector
MUC1 siRNA
kDa
0 6 12 0 6 12 h ICI
65-
ERα
IB: anti-ERα
43-
β-actin
IB: anti-β-actin

A.

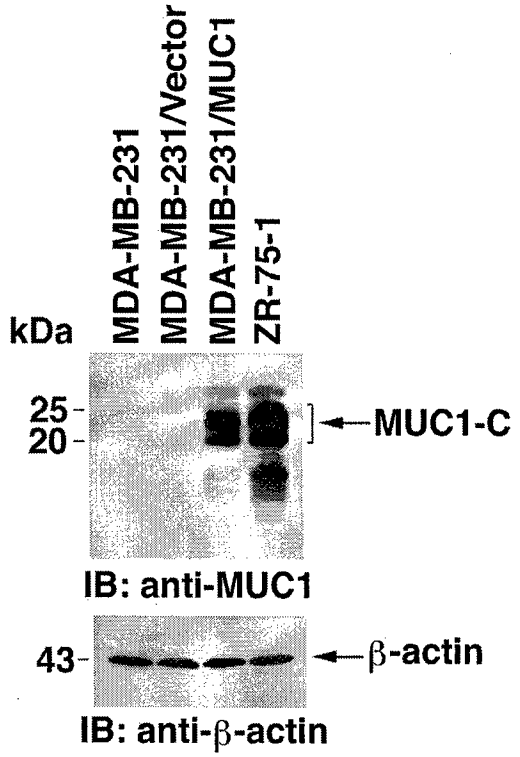
MDA-MB-231
MDA-MB-231/Vector
MDA-MB-231/MUC1
ZR-75-1
kDa
25
20
MUC1-C
IB: anti-MUC1
43
β-actin
IB: anti-β-actin

B.

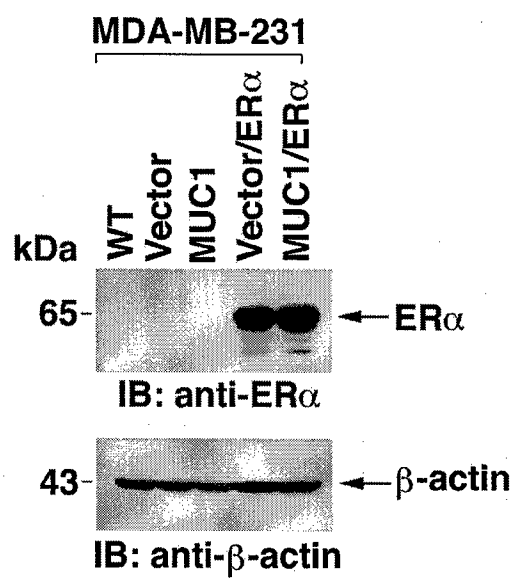
MDA-MB-231
WT
Vector
MUC1
Vector/ERα
MUC1/ERα
kDa
65
ERα
IB: anti-ERα
43
β-actin
IB: anti-β-actin

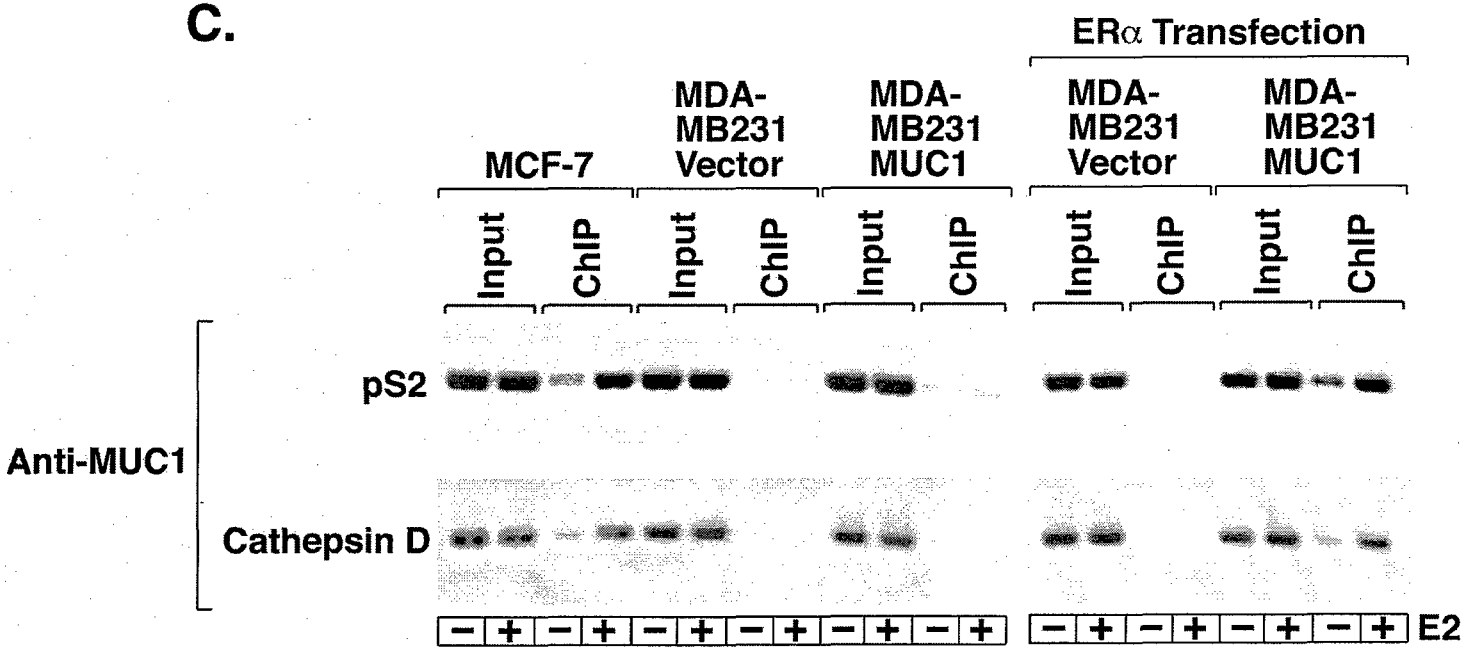
C.
ERα Transfection
MCF-7
MDA-MB231 Vector
MDA-MB231 MUC1
MDA-MB231 Vector
MDA-MB231 MUC1
Input
ChIP
Input
ChIP
Input
ChIP
Input
ChIP
Input
ChIP
pS2
Anti-MUC1
Cathepsin D
− + − + − + − + − + − + − + − + − + − + E2

A. MCF-7

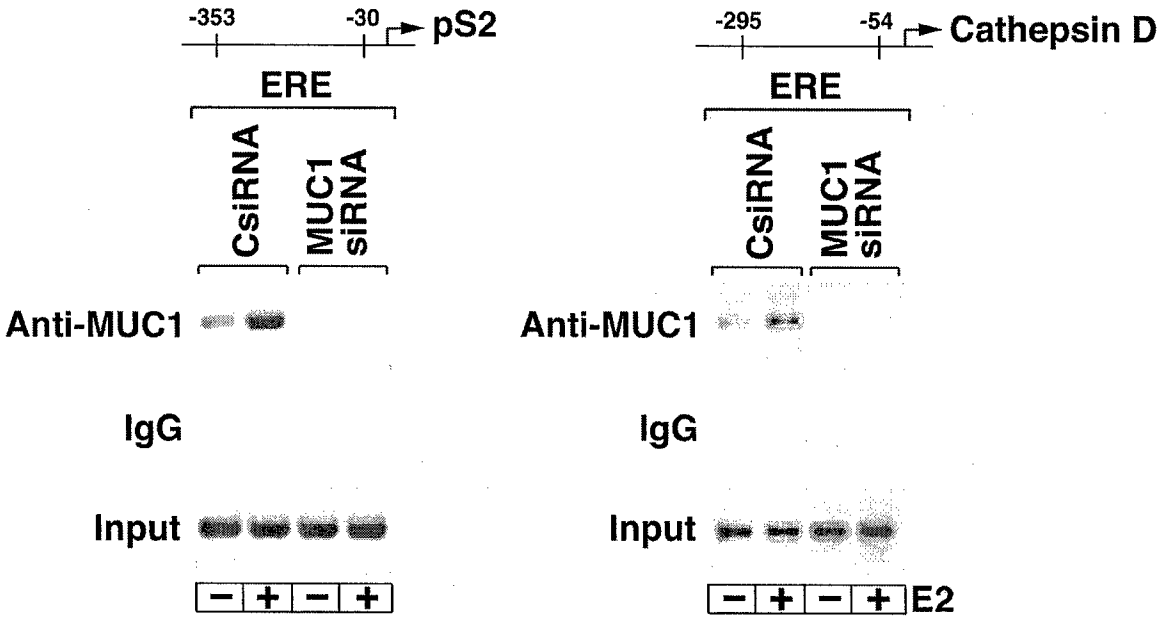
-353
-30
pS2
ERE
CsiRNA
MUC1 siRNA
Anti-MUC1
IgG
Input
− + − +
-295
-54
Cathepsin D
ERE
CsiRNA
MUC1 siRNA
Anti-MUC1
IgG
Input
− + − + E2

B. MCF-7

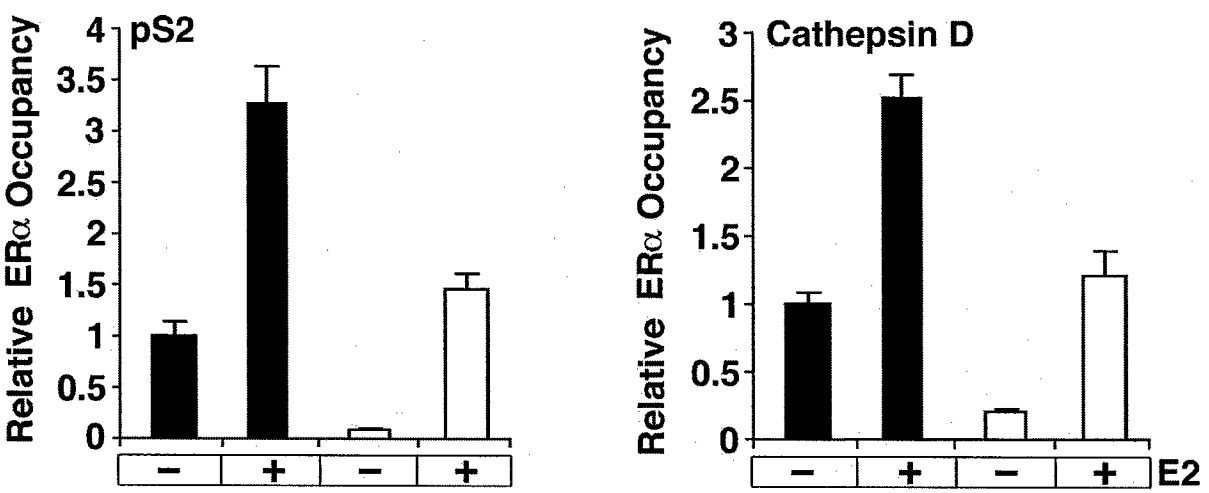
Relative ERα Occupancy
4
3.5
3
2.5
2
1.5
1
0.5
0
pS2
− + − +
Relative ERα Occupancy
3
2.5
2
1.5
1
0.5
0
Cathepsin D
− + − + E2

C. ZR-75-1

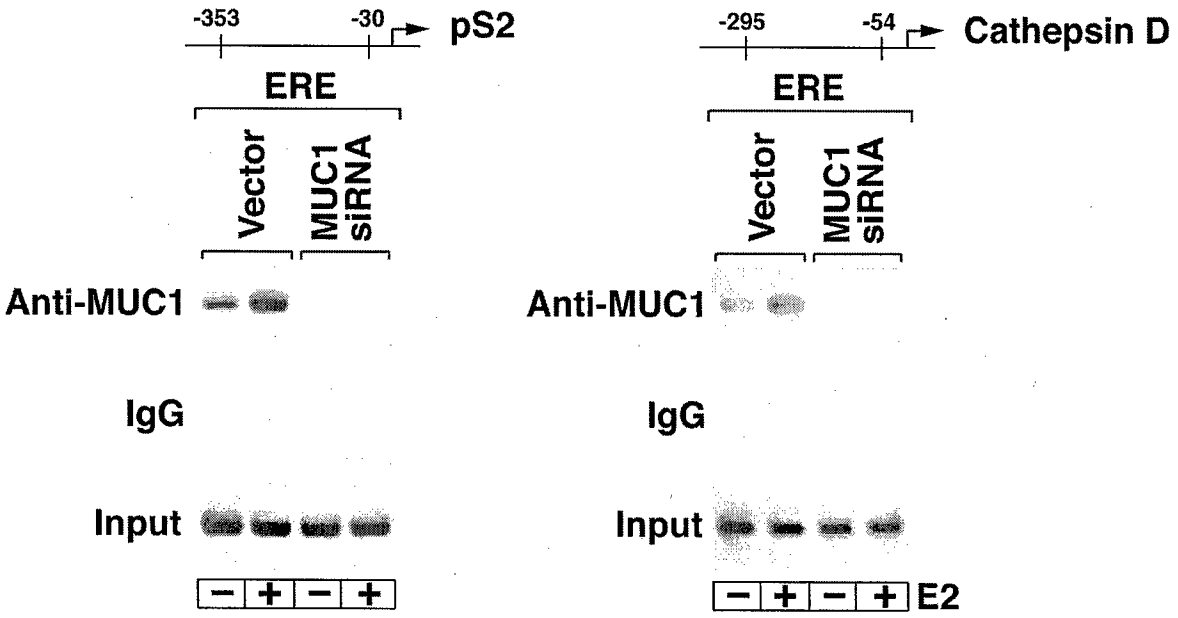

D. ZR-75-1

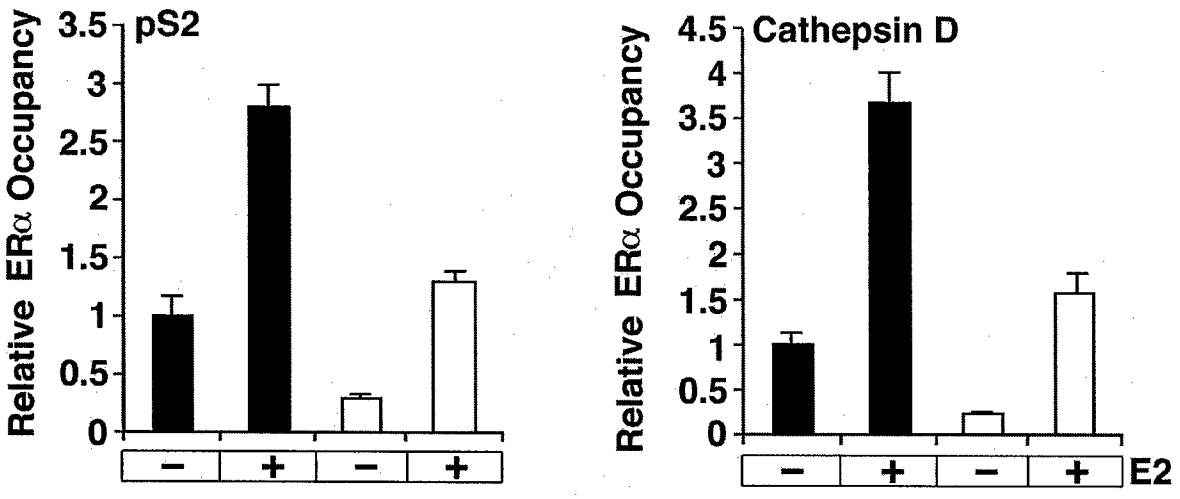

Fig. S6AB

A.

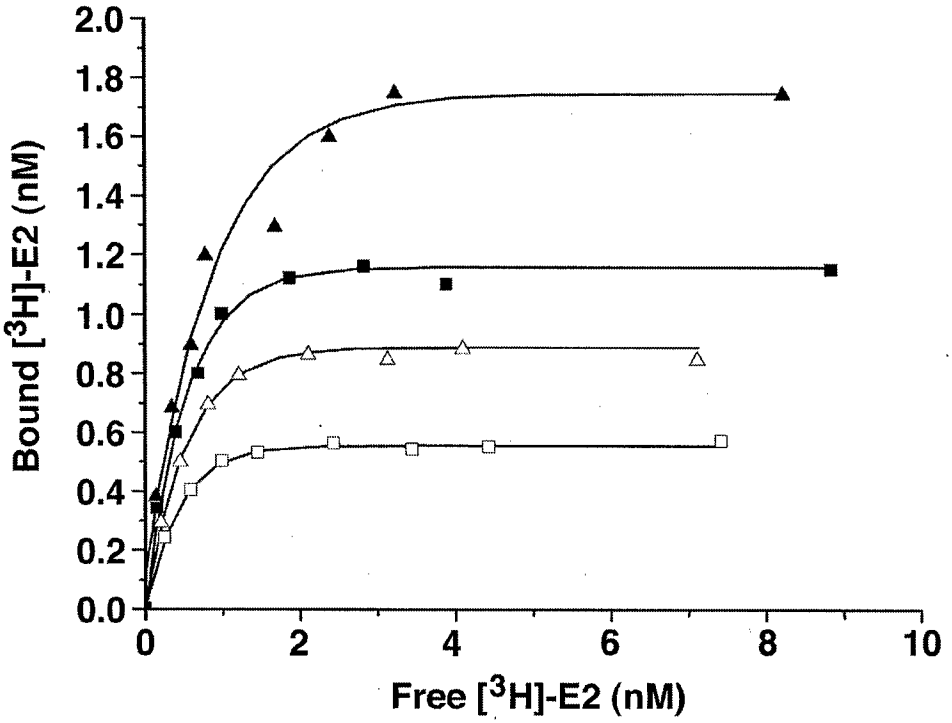
Bound [3H]-E2 (nM)
2.0
1.8
1.6
1.4
1.2
1.0
0.8
0.6
0.4
0.2
0.0
0
2
4
6
8
10
Free [3H]-E2 (nM)

B.

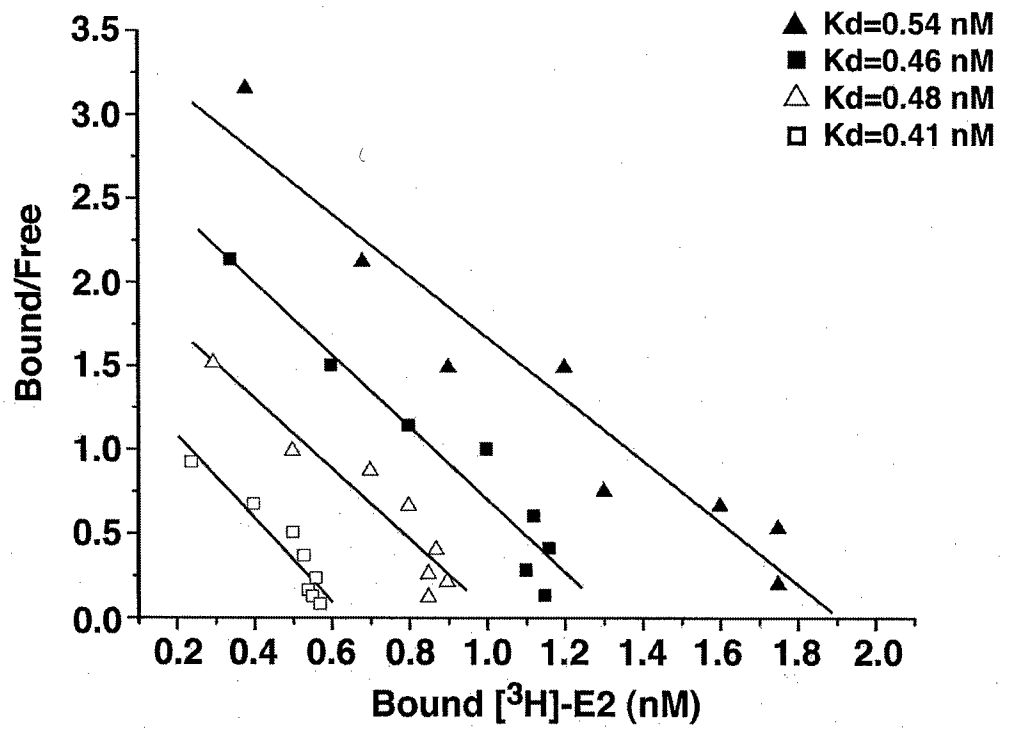
Kd=0.54 nM
Kd=0.46 nM
Kd=0.48 nM
Kd=0.41 nM
Bound/Free
3.5
3.0
2.5
2.0
1.5
1.0
0.5
0.0
0.2
0.4
0.6
0.8
1.0
1.2
1.4
1.6
1.8
2.0
Bound [3H]-E2 (nM)

Fig. S6CD

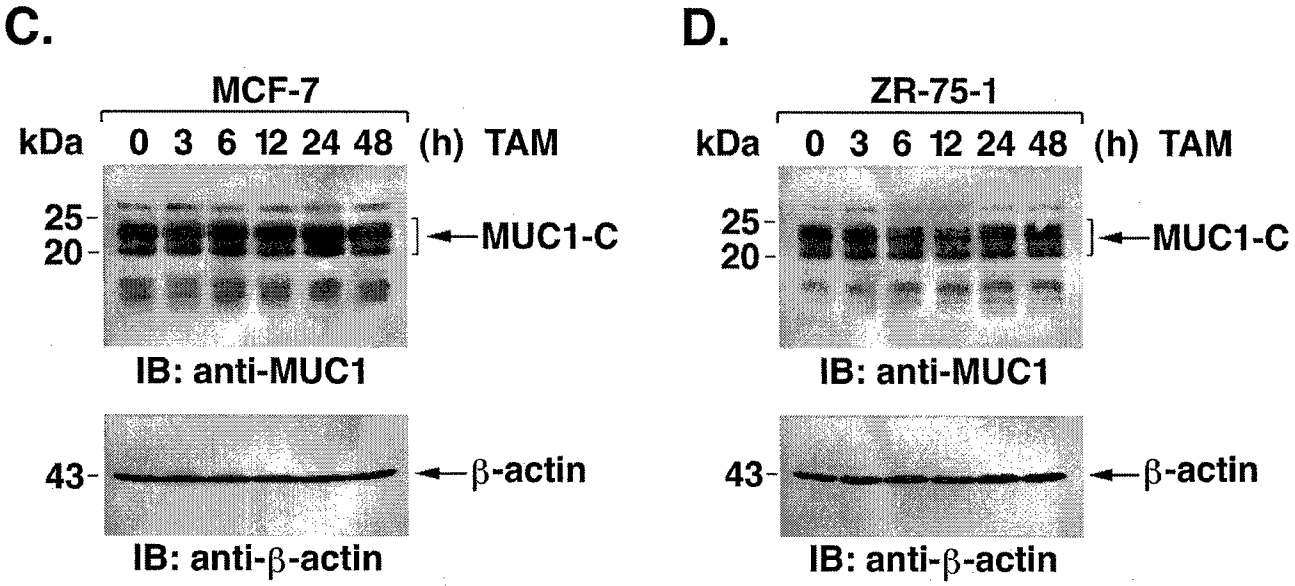
C.
MCF-7
kDa 0 3 6 12 24 48 (h) TAM
25-
20-
MUC1-C
IB: anti-MUC1
43-
β-actin
IB: anti-β-actin
D.
ZR-75-1
kDa 0 3 6 12 24 48 (h) TAM
25-
20-
MUC1-C
IB: anti-MUC1
43-
β-actin
IB: anti-β-actin

Fig. S7AB

A. MCF-7

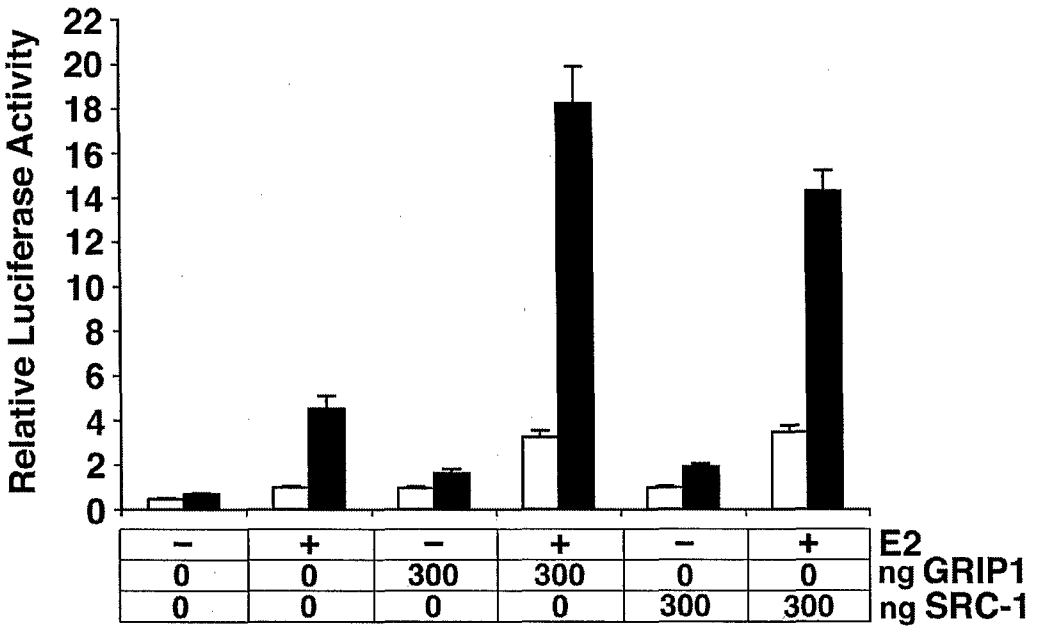

B.

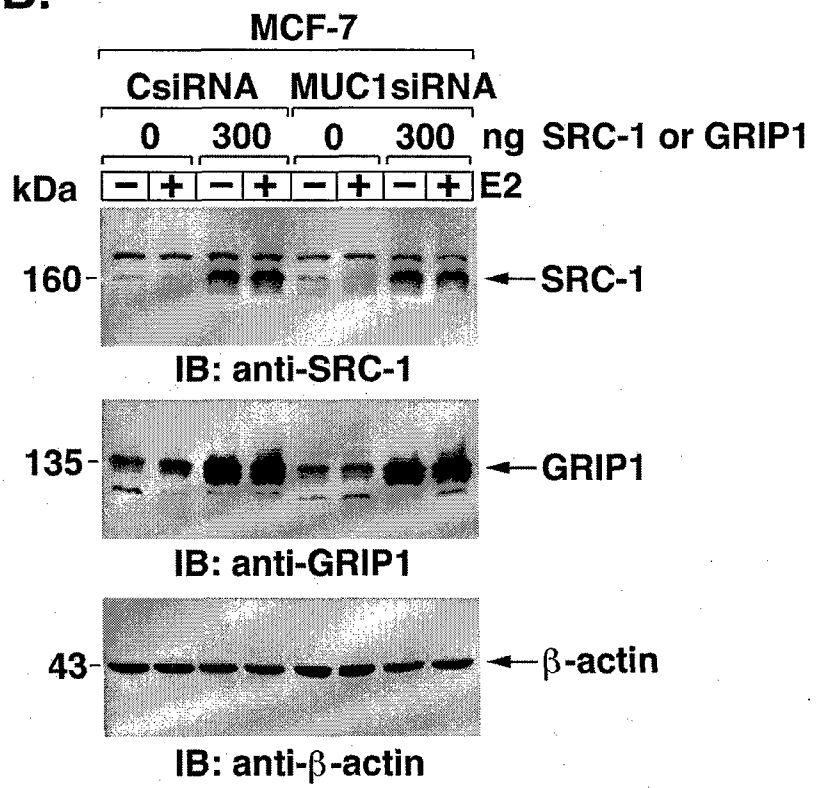

C. ZR-75-1

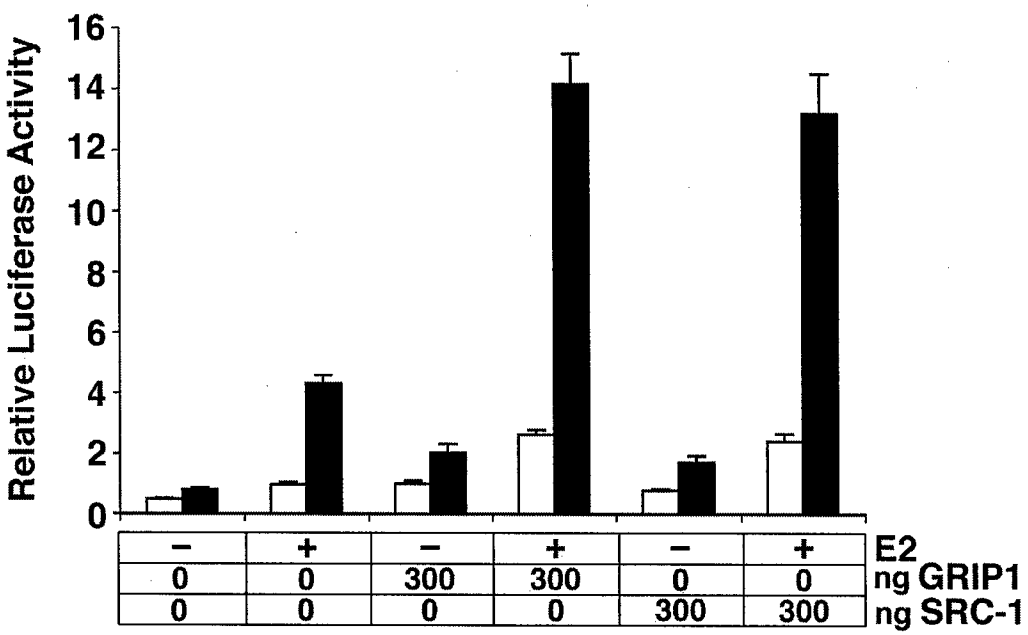
Relative Luciferase Activity
16
14
12
10
8
6
4
2
0
– + – + – + E2
0 0 300 300 0 0 ng GRIP1
0 0 0 0 300 300 ng SRC-1

D.

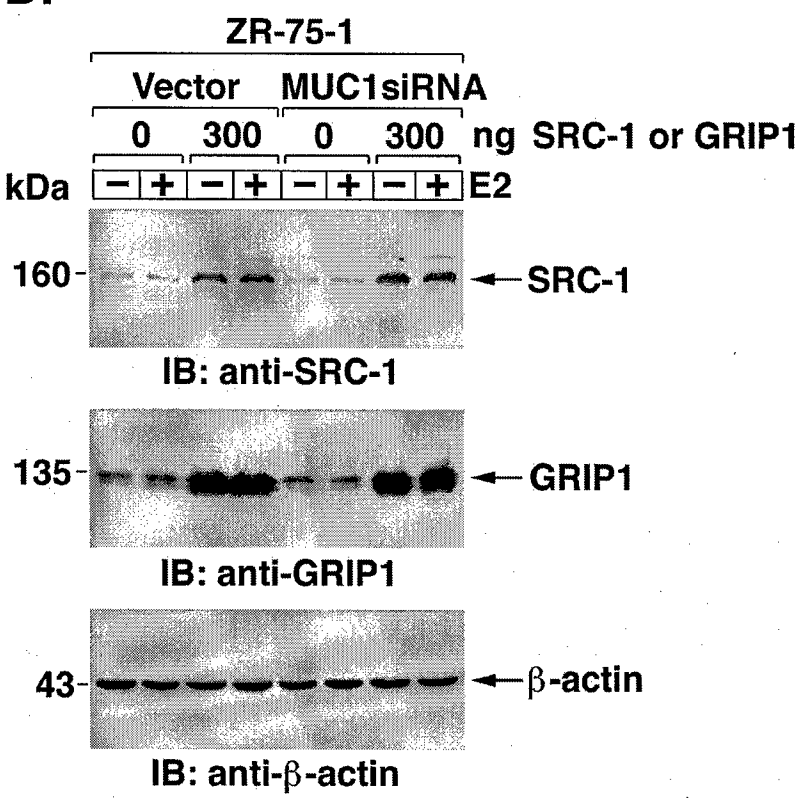
ZR-75-1
Vector
MUC1siRNA
0 300 0 300 ng SRC-1 or GRIP1
kDa
– + – + – + – + E2
160
SRC-1
IB: anti-SRC-1
135
GRIP1
IB: anti-GRIP1
43
β-actin
IB: anti-β-actin